RESPONSE OF ADHESIVELY BONDED COMPOSITE JOINTS TO LOW VELOCITY IMPACT

A Thesis by

Govind Ramakrishna Pillai

Bachelor of Technology, University of Kerala, India, 2001

Submitted to the Department of Mechanical Engineering
and the faculty of Graduate School of
Wichita State University
in partial fulfillment of
the requirements for the degree of
Master of Science

December 2006

RESPONSE OF ADHESIVELY BONDED COMPOSITE JOINTS TO LOW VELOCITY IMPACT

I have examined the final copy of this thesis for form and content and recommend that it be accepted in partial fulfillment of the requirements for the degree of Master of Science, with a major in Mechanical Engineering.

_____

Hamid M. Lankarani, Committee Chair

We have read this Thesis

And recommend its acceptance

_____

Bob Minaie, Committee Member

_____

Krishna K. Krishnan, Committee Member

DEDICATION

To God and my parents

ACKNOWLEDGEMENTS

I would like to present my sincere gratitude towards my graduate advisor, Dr. Hamid Lankarani for his continuous support and guidance in completing my thesis. I would also like to thank Dr. Bob Minaie and Dr. Krishna K. Krishnan for reviewing my thesis and making valuable suggestions.

I would like to express my deepest gratitude to Mr. Waruna P. Senerviratne, Manager of the Structures Laboratory, at the National Institute for Aviation Research (NIAR) for his vision, expertise, patience and guidance throughout the entire project. I would also like to express thankfulness to Mr. Soohan Loo, Manager of the Thermal & NDI Department for providing me with testing equipment and supporting me to a wider extend for completing the experimental study.

I would like to thank my family, my father, M. Ramakrishna Pillai, my mother, Suma Ramakrishnan, my sister, Gopika Krishnan for always being there for me providing me with encouragement for pursing my educational goals and standing by my side throughout my entire life.

I am indebted to my many colleagues and friends for providing a stimulating and fun environment to learn and grow. I would like to appreciate the valuable help provided by my friends from Wichita State University; especially Vinay Bhamare, Amit Yeole, Anand B. Despande, Neebu Alex Urban and Santhosh Kumar for helping me to get through difficult times and for their emotional support, entertainment and caring.

Finally, I would like to thank all the direct and indirect supports that helped me complete this thesis.

ABSTRACT

Adhesively bonded composite joints are widely used in modern lightweight flight and space vehicle structures and will be widely used in the next generation aircrafts such as Unmanned Aerial Vehicles (UAV) and Joint Strike Fighters (JSF). Designing of adhesively bonded composite joints is a challenging task as the characteristics of the composite laminate adherends have an effect on their performance. Wide use of composite materials is attributed to their superior properties such as high specific stiffness, excellent fatigue properties as well as resistance to environmental conditions. Although they possess such superior properties, their relatively low through thickness strength and susceptibility to impact have a significant concern preventing designer from using in areas which are prone to impact damage.

In this experimental study, impact testing was done on adhesively bonded composite laminates. Hysol EA 9394 was the adhesive used for bonding the composite laminates. Glass/Epoxy, Carbon Plain Weave/Epoxy and Carbon Unitape/Epoxy were the composite laminate adherends used for the formation of the lap joint. Quasi-isotropic laypup sequence was used for manufacture of the composite adherends. Lap joints formed using the above said adherends were impacted at the center of the joint using an Instron Dynatup drop tower with impactors of different diameters as well as with different energy levels. The impacted specimens were then non-destructively inspected using through transmission ultrasonic C-scan. Residual indendation on the impacted specimen is also recorded.

Impact force, total energy absorbed, duration of impact and impactor displacement were the important parameters which were used to quantify impact response of the adhesively bonded composite joints. In addition to the above said parameters, damage area obtained from through transmission ultrasonic C-scanning was also used to quantify the impact response of the

adhesively bonded composite joints. Residual indentation measurement combining with visual inspection was made use for preliminary damage detection.

TABLE OF CONTENTS

TABLE OF CONTENTS (continued)

LIST OF TABLES

LIST OF FIGURES

LIST OF FIGURES (continued)

LIST OF FIGURES (continued)

LIST OF FIGURES (continued)

Figure Page

CHAPTER 1

INTRODUCTION

1.1 Background

Composite materials are usually, three-dimensional combinations of at least two chemically distinct reinforcing materials such as carbon or glass fiber, with a distinct interface or matrix separating the components. These materials are usually constituted to obtain properties that cannot be achieved by any of the components acting alone.

The increasing requirements for stiff light weight structures, especially in the aerospace, automobile and marine industries has led to a great increase in the use of fiber reinforced composite materials, as they have a high strength-to-weight ratio and specific stiffness when compared to metals. In aircrafts, composite joints are rapidly replacing fasteners and rivets which are generally employed in aircraft structures. Despite of the advantages possessed by composite materials, they do have some limitations such as susceptibility to damage brought on by low-velocity impacts with various objects such as hail, bird strikes, runway and taxiway rubble or even dropping of tools during manufacture. These limitations are especially acute in regions where individual composite components are joined together by fasteners, riveted joints or by adhesive joints as joints are areas prone to strength reduction. In the present age of improving fuel efficiency without compromising on the strength of structure, adhesive joint proves to be a forerunner compared with riveted joints or fasteners. Of the various advantages possessed by adhesive joint over other forms of joints, adhesive bonding increases the strength of the joint as stresses are evenly distributed because of larger surface area of contact. This being the case, the response of joints especially the most prevalent form of composite joints – the adhesive joint to

low velocity impact should be understood in detail before incorporating these composites into aircraft structures.

1.2 Statement of Work

Impact tests are very difficult to understand because of numerous parameters which play an important role in an impact event. Degree of complexity of an impact event on fiber reinforced composites is higher because of the heterogeneous behavior as well as anisotropic nature of composite materials and also due to the complex failure modes that can occur. Understanding the process of impact damage initiation and growth and identifying the governing parameters are important for designing impact resistant structures and for developing improved material systems. The objective of this research is to study the response of adhesive joints in various fiber reinforced composite panels to low velocity impact for different energy levels, and various impactor diameters and for different materials based on impact energy, damage area and residual indentation. This being so, some of the primary areas of interest for this study are as noted below:

- Impact Testing
- Failure modes in low –velocity impact damage
- Experimental Methods for assessing damage

CHAPTER 2

LITERATURE SURVEY

2.1 Adhesives

An adhesive can be defined as a material which when applied to surface materials can join them together and resist separation. Although, adhesives have been used by humans for thousands of years in their drive to make objects stronger and more useful, it is hard to quote a single moment when their usefulness was first discovered. Instead, use of adhesives is likely to have been a gradual process. As commented by Alexander (1923), 'the real glue and gelatin industry emerged about the beginning of the nineteenth century'. In these early days of industrialization, quality control was almost non existent in glue factories and the final products available for use were of varying quality and performance. Involvement of scientific discipline to glue industry made possible the much required documentation of available knowledge regarding glue manufacture as well as the testing results. By the beginning of 20^{th} century, testing of manufactured glue products not only did influence the performance and quality of the glues but it greatly influenced the market value of the glue. The development of test methods during the early 20^{th} century paved way for many of the test methods in use for assessing uncured adhesives as well as the strength and durability of the adhesive joints.

The creation of epoxy resins could be considered as the single most important landmark in the history of structural adhesives. Epoxy based adhesives was successfully employed in aerospace, automotive, construction, electronic and woodworking applications largely because of their ease of use, versatility and mechanical properties. Epoxy adhesives possess high shear strength but relatively low toughness and peel strength. Adhesives can be classified in the manner in which they harden. Common ways in which adhesives harden are either by loss of

solvent, loss of water, cooling or chemical reaction. Crosslinking of the polymers happen during hardening which usually happens in structural adhesives [1].

2.2 Bonded Joints

Joint design is dependent on the nature of materials to be joined as well as the method of joining. The load bearing structural adhesive joint can be considered relatively new, about half a century old. A structural adhesive is provides major strength and stiffness for the structure preventing the joint from separation under load. Joints could be obtained either by fastening the surfaces by either by mechanical fastening methods or by using adhesive bonding. Various factors are to be considered while using adhesive bonding for joints such as whether the structure need to be dismantled for repair, maintenance or inspection, how the assembly is affected, and in what environment is the assembly going to function which are a few major factors to be considered while using adhesive bonding. As dismantling and reassembling of adhesively bonded structures is almost impossible with such structures it's always economical as well as effective to use adhesive bonding for subassemblies which could be designed as throw away parts which does not require dismantling.

Utilization of adhesive joints depends on the development of structural materials especially in aerospace industry as bonded joints are present vastly in that industry. Adhesive bonding is advantageous compared to mechanical joining as the former as they have higher fatigue and corrosion resistance together with superior strength when thin sheets of materials are bonded together. Bolts or rivets could be considered as points of high stress concentration that can lead to structures having lower static and fatigue strengths than an adhesive bonded system. On the darker side, adhesive bonded joints require extensive surface preparation as well as they have poor resistance to environmental degradation. As for composite materials surface

preparation requirements are minimal, such joints are more feasible in composite materials. Design of bonded joints is an iterative process which involves stress analysis, suitable failure criteria, environmental effects and manufacturing process for determining suitable joint configuration and materials [6]. Typical joint configurations are shown below in Figure 1.

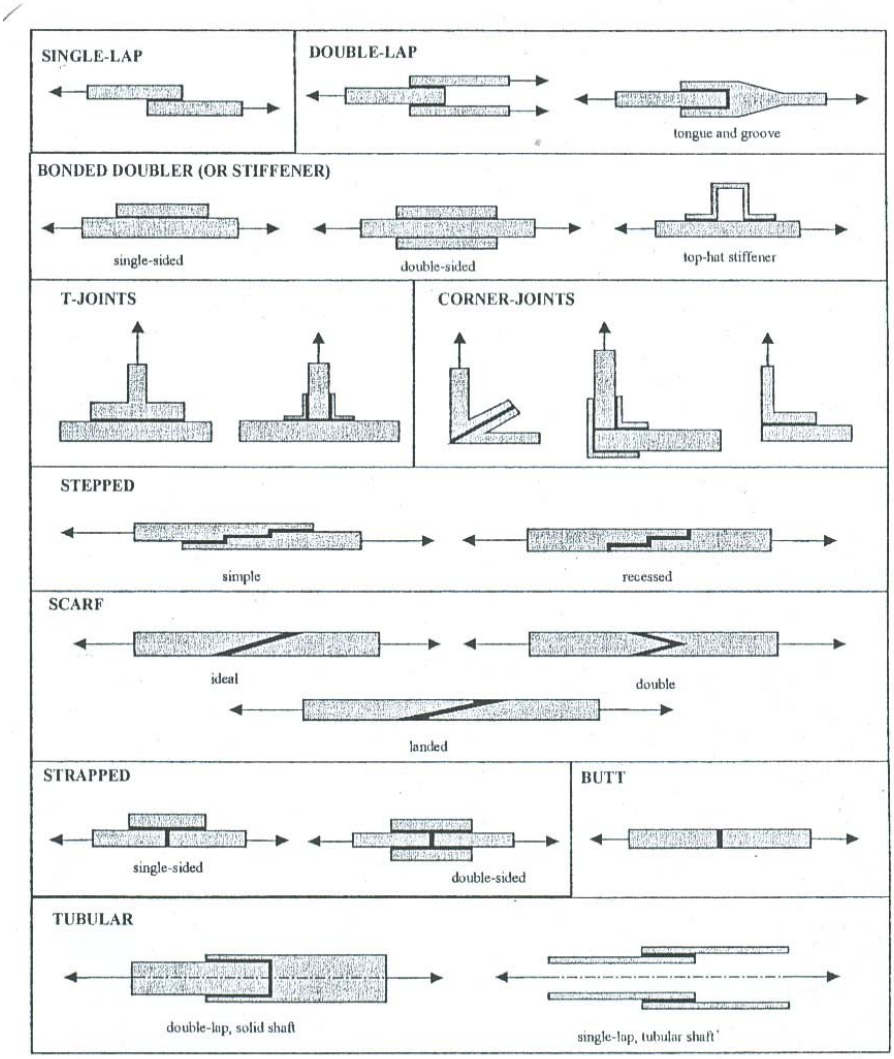

Figure 1. Typical joint configurations [6].

The single lap joint could be considered as one of the most common 'plate-to-plate' joint designs employed in the industry as its easy and cheap to manufacture. When it comes to inspection of the joint, it's the most convenient one for inspection as complete inspection can be

made from one side of the joint. Under tension this joint poses a problem which is often used to demonstrate the accuracy of theories for calculating the stresses in adhesively bonded joints.

Ashcroft et al. [7] investigated the effects that environment and fatigue loading have on the performance of bonded composite joints. Studies were mainly concentrated on the environmental effects – both prior to and after bonding. It was concluded from their investigation that temperature and humidity have a considerable effect on the mechanical performance and the nature of failure process. From their investigation, it can be comprehended that at higher temperatures, the strength of short overlap joints is controlled by the yielding and flow behavior of the adhesive rather than by its fracture resistance. It is also inferred from their work that moisture contained prior to bonding resulted in formation of voids in the bondline which results in the strength of the joint. An interesting observation from their research work is that upon drying a substantial proportion of initial strength could be regained which indicated that plasticization of the composite matrix or adhesive because of moisture is a reversible process.

Mechanically fastened components can sometimes show fretting due to very small amplitude relative movement normal to their mating surfaces when vibration is transmitted through the joints. Adhesive bonding can serve to damp or attenuate the vibration and also it can eliminate the fretting. Vibration could also loosen the bolted assemblies. To prevent this, thread locking adhesives are used for prevention [2].

2.3 Impact Testing

Impact resistance is the study of damage induced by foreign object impact in a laminate and the factors affecting it. An understanding of impact damage development, the failure modes involved, and the various factors affecting damage size can be gained only through extensive experimental studies. Of the different techniques discussed in the literature, some were

nondestructive and others are destructive. To simulate actual impact by a foreign object, a number of test procedures have been suggested. Special consideration is given for initial kinetic energy of the projectile as it is an important parameter to be considered but several other factors also affect the response of the structure. Abrate [4] quotes that a large mass with low initial velocity may not cause the same amount of damage as a smaller mass with higher velocity even if the kinetic energies are exactly the same. In one case, the impact might induce an overall response of the structure, while in the other the response might be localized in a small region surrounding the point of impact. Hence it can be inferred from the experiments conducted by the author that appropriate test procedure selected so as to ensure that the test conditions are similar to the impact conditions to be experienced b y the actual structure.

Experimental studies attempt to replicate the actual situations under controlled conditions. Many procedures have been contrived to assess the impact performance of adhesively bonded joints because of the wide variety of applications. The various methods used for quantify the impact behavior are provided in the succeeding section.

2.3.1 Pendulum Test

In a pendulum test, a small block is adhered to a larger block which is fixed to the base of the testing machine and an impact load is applied to the small block due to the collision of the pendulum hammer. At impact, the joint is subjected to high rate shear loading and is fractured. Impact energy absorbed by the joint specimens can be calculated from the difference of the pendulum height between the initial position before the test and its maximum height after the collision [1].

2.3.2 Dropweight Tester

Drop weight testers are extensively used and can be off differing designs. Heavy impactors are usually guided by a rail during their free fall from a given height. Usually a sensor activates a mechanical device designed to prevent multiple impacts after the impactor bounces back [1]

2.3.3 Split Hopkinson Bar (Kolsky Bar)

Pendulum tests and drop-weight tests are ineffective in achieving high strain rates. In- order to achieve higher strain rates, i.e., strain rate of 10^2/s - 10^3/s, usually Split Hopkinson bar technique is often used. Using Split Hopkinson bar technique strain rate of 10^2/s - 10^3/s can be realized easily and using special experimental setups higher strain rates upto 10^4/s could be obtained. Typical Hopkinson bar equipment is used for impact compression tests; it has two steel bars which are the input bars and output bars between which a specimen is inserted. A striker, which is accelerated usually with a gas gun, collides with the end of the input bar to cause a stress wave in the bar and the wave reaches and transmits the specimen as an impact load [1].

During aircraft take off and landing, debris flying from the runway can cause damage; this situation with small high velocity projectiles is best simulated using a gas gun. Another concern is the impact of a composite structure by a larger projectile at low velocity which occurs when tools are accidentally dropped on a structure. This situation is best simulated using a drop weight tester [4]

During the impact by a spherical projectile, the stress distribution under the impactor is truly three dimensional. As soon as the projectile enters in contact with the target, a compressive wave a shear wave and surface waves propagate away from the impact point. For low velocity

impacts, no significant damage is introduced during the early stage of the impact. That is stress levels remain low as these waves travel many times through the thickness of the laminate and then the target deforms like a plate. Damage is introduced when overall bending motion is established. With higher velocity impacts, the compressive wave after reflection from the back surface can generate tensile stresses of sufficient magnitudes to create failure near the back face [4].

2.4 Low Velocity Impact Testing

Feraboli et al. [9] showed that peak force cannot be always considered as a criterion to compare impact events. They have quoted that peak force should not always be used to for assessing damage maps. They also found out that there is a critical value of impact force for damage initiation which is independent of impact energy. An experimental database is generated through drop tower impact testing of an undeformable striker on clamped circular plates, for a particular composite material with a particular layup sequence and laminate thickness. From these experiments conducted, they have concluded that critical force rather than peak force should be used to characterize damage resistance of composite structures.

Belingardi and Vadori [13] [18] studied the low velocity impact behaviour of carbon fiber-epoxy matrix laminates using drop dart tests. Composite laminates of two different stacking sequences, different laminate thicknesses were tested both by quasi-static and dynamic impact loading. It can be found out from their research that as expected the global energy absorption increases as the number of layers increase. Degree of damage was the most relevant parameter in this study. It could be seen that there exists a trend in damage degree with respect to specific impact energy. The damage degree is increasing until the saturation of the material. The force versus displacement curves shows that the values of first damage force and maximum force

values remain substantially constant with impact energy which implies that these parameters depend on the laminate thickness.

Farrow et al. [16] conducted study on the effect impact on adhesively bonded single lap composite joints. Low velocity impacts were conducted at very low energy levels so that the damage made on the joint is barely visible. Results show that in the top laminate, delamination occurs at the interface between 0^0 layer and 45^0 and 90^0 layers. In the adhesive, cracks at 45^0 indicate typical shear failure. In the bottom laminate, delamination between layer interfaces exists but increase through the depth at an increasing rate compared to that in the top laminate. The authors comments on the adhesive-laminate interface during the tensile testing. It was found that the interfaces were intact in all specimens after failure which suggests that the joint failure maybe due to the adherends and not due to the adhesive.

Ambur and Kemmerly [19] conducted an experimental study on the effect of the impactor mass on the low-speed impact response of laminated flat composite plates. It has been shown from the available test data that the compression strength of composite structures can be significantly reduced by the damage induced by low – velocity impact. 48-ply-thick quasi – isotropic flat plate test specimens were used for their experimental study. Energy levels varied from 7.5 ft-lbs to 25 ft-lbs and the impactor weights ranging from 2.5 to 20.0 lbs and an impactor diameter of 0.5-inch was used for the study. As the Impact energy increases due to the damage initiation, there is reduction in the contact force and respectively there is a change in the damage modes in the specimens. It is also found that with increase in mass of the impactor results in a reduction in the damage area.

Hosur et al. [20] conducted a study on the impact response of woven fabric laminates manufactured by affordable VARIM process under low velocity impact loading. Plain and satin

weave graphite fabric laminates were used for the experiments and impact tests were conducted with energies ranging from 5 to 40 J. Ultrasonic C- Scan techniques was used for the non destructive examination of the damage induced on the specimens. Regarding the failure mechanisms, its different in woven fabric composites as compared to unidirectional laminates. It has been observed that 8-harness stain weave fabric laminates showed better impact resistance through higher peak loads, higher stiffness and lower damage area.

2.5 Experimental Methods for Damage Assessment

Impact on fiber reinforced composite laminates can be characterized with parameters such as impact energy, impact force. Evaluating the impact behavior using those parameters would not be complete without finding out the damage induced in the fiber reinforced composite laminates. Damage measurement in composites can classified as non-destructive testing and destructive testing. During an impact event, the damage is internal and generally consists of delamination, matrix cracking and fiber breakage. This makes it very difficult of measure the damage as surface examination cannot tell completely about the damage induced in the laminate.

2.5.1 Non Destructive Techniques

Non destructive testing is now an essential part of quality assurance in many areas such as manufacturing industry, construction industry, process or quality control, maintenance and also in medical industry too. The basic principle of non-destructive testing is very straightforward – to determine the quality or integrity of an item non destructively, find a physical phenomenon that will interact with and be influenced by the test specimen without altering the specimen's function. The basic guidelines in choosing an NDT method is by understanding the physical nature of the material property or discontinuity o the material to be

inspected, understanding the physical nature of the interaction of the probing field with the test material as well as considering the economic, environmental as well as regulatory factors[5]. All non destructive testing methods are based on physical principles. Basic principle of non-destructive testing is subjecting the specimen being examined to some form of external energy source and analyzing the detected response signal. Non destructive testing relies completely on the full understanding of the response of materials to different types of external stimuli and on the ability to analyze the response signal compared to the predicted theoretical behaviour. The different types of non-destructive testing methods which are used for various purposes such as research, maintenance are described below [5].

2.5.1.1 Liquid Penetrant

Penetrant testing is a very simple and a sensitive non destructive testing method. Rather than being simple, this method is an inexpensive as well as a quick method for inspection of a large variety of component parts and materials for discontinuities that are open to the surface. Basic principle of penetrant testing is the ability of the penetrant fluid to coat the specimen completely, and then to penetrate the depths of the discontinuities open to the surface. For detection of the defects using this method, the indicator material must be visible. Hence proper illumination is required for efficient use of this method. This method of testing is advantageous in many aspects, could be utilized in various industries, convenient portability of equipments for testing, could be used irrespective of the size and shape of the specimens to be tested. The handicap of this test is that it requires an experienced inspector and also this test can detect only defects that are open to the surface of the specimen [5]

2.5.1.2 Ultrasound

Non-destructive testing using ultrasonic could be considered as the most widely used methods used in industry. Ultrasonic waves are high frequency sound waves which vibrate at a frequency above 20,000 Hz. In ultrasonic inspection, a transducer transforms a voltage pulse into an ultrasonic pulse. A transducer transmits the pulse into the test object and the pulse travels through the object with respect to the geometry and mechanical properties. The coming through the specimen is then transmitted to another transducer or reflected back to the original transducer. In both methods, the signal is transformed back into an electrical pulse which can be observed in an oscilloscope. Based on the signal, presence of a flaw, defect or delamination and its size, shape, position and composition could be detected without much difficulty. Non-destructive testing using ultrasonic find innumerable applications in the aircraft, semiconductor as well as medical industries. Ultrasonic methods are advantageous as it could be used to test complex geometries irrespective of materials. It could be used for metals to ceramics to biological materials. Ultrasonic methods offer contacting as well as non contacting approaches. Like all non destructive testing methods, this method also requires experienced personnel for effective use of the method. In all cases, ultrasonic methods require the transducer to be in contact with the object through water or a gel-coupling layer. Capability to reveal planar flaws is almost absent in ultrasonic waves [5].

2.5.1.3 Magnetic Particle Inspection (MPI)

Magnetic particle inspection is one of the most economical for detecting defects in a ferromagnetic material. In this method, the sample is magnetized and simultaneously finely divided ferromagnetic particles are flown over the surface. Any defects in the materials will affect the magnetic field in the sample and which will attract magnetic particles to the edges of

the defects. MPI is simple to operate as well as to interpret, reliable for finding surface cracks, it could detect the defect even if the defect is filled with some foreign body such as thin coats of paint or plating. MPI is limited to ferromagnetic parts and also it can detect only surface or near surface cracks [5].

2.5.1.4 Acoustic Emission (AE)

Acoustic emission is a passive monitoring method, in which acoustic energy released by the material or the structure is monitored while the structure is under load. The initiation or propagation of damage mechanisms produce acoustic waves which help in detection as well as assessment of damage mechanisms. Acoustic emission can be defined as the release of transient elastic waves produced by a rapid distribution of stress in a material. Measurement of AE waveforms depends on the generation of the waveform at the source, propagation and measurement. Acoustic emission is a vastly developing technique which is finding application in various areas. This method finds its major application is damage activity monitoring, detecting damage location, identifying the damage mechanism as well as strength predictions. Using an array of sensors, arrival times of the acoustic emission at different sensor locations combined with the acoustic wave speed help to identify the position of the source. Once the damage area is detected, other non destructive testing methods can be utilized to find out the severity of the damage. Attempts have been made to estimate the residual strength of a structure using Acoustic emission method. Such a calculation is difficult as there is no physical link existing between strength and acoustic emission as all non destructive testing uses some physical phenomena to bring out results [5].

2.5.1.5 Active Thermography

Active thermography uses infrared imaging with the help of external heating to evaluate subsurface structure. It makes use of the thermal response of the sample. Active thermography focuses on the detection of subsurface structures and defects utilizing the variation in thermal properties between the defect and the host material. Active thermography uses an infrared camera which allows images of the surface temperature distribution of a sample to be taken in video rates. In this method, sample to be tested is heated with a modulated light source and the temperature distribution is recorded with the infrared camera as a function of time [5].

Various other methods of non destructive testing used for the evaluation of damage are using microwaves and optical techniques such as holographic interferomety, speckle techniques and photoelastic techniques.

Destructive techniques include sectioning of several strips of material at different locations and orientations throughout the impacted zone. These strips are then mounted in epoxy resin and ground on successively finer abrasive silicon carbide paper. After that each strips are examined carefully under microscope to construct detailed maps of delaminations at each interface and of matrix cracks in each ply.

CHAPTER 3

MATERIAL SELECTION AND SPECIMEN FABRICATION

3.1 Material Selection

Composite joint, which is the main area of interest in this study, was fabricated using woven glass/epoxy, carbon/epoxy plain weave fabric and carbon/epoxy unidirectional tape adherends and the adhesive used for bonding of these adherends is Hysol EA 9394 which is an epoxy paste adhesive. Material selection and adhesive selection was carried out by taking into consideration of an actual joint which is employed in industry. Utmost care was taken in the selection of materials as well as adhesive as these could be said as the major factors which play a very important role in the whole investigation Woven glass/epoxy adherend was used to simulate the joints which exists in small aircrafts as well as used in marine applications. As this material is translucent, visual observation of the internal damage is also possible.

Materials which were selected for this study were in the form of prepregs which is an abbreviated usage for fibers impregnated with resin. Basic information regarding the materials which were used for this study is listed in Table 1.

TABLE 1

BASIC PREPREG INFORMATION

MANUFACTURER	FIBER PRODUCT ID	RESIN PRODUCT ID	MATERIAL IDENTIFICATION
NEWPORT	7781	NB 321	E- GLASS/ EPOXY WOVEN
TORAY	T700G-12K-PW	3900-2	CARBON/ EPOXY PLAIN WEAVE FABRIC
TORAY	T800S	3900-2B	CARBON/EPOXY UNIDIRECTIONAL TAPE

After material selection, layup sequence for the laminates as well as the specimen geometry has to be taken care of. Severity of the damage that is going to be induced in the composite laminate during impact loading as well as thickness of the specimen decides the layup sequence. In order to have sufficient strength for the joint, in this experimental study, quasi isotropic layup sequence is employed. Composite laminates were fabricated using hand layup and cured in autoclave in accordance with the cure cycle mentioned by the manufacturer.

3.1.1 Glass Adherend

Glass adherend used for the experiment study is Newport NB 321 with style 7781 woven fiber glass. Newport 321 is a 250°F to 300°F cure, toughened, high T_g, controlled flow epoxy resin system. High T_g and excellent mechanical properties make it an ideal product for general aviation as well as aviation market. Layup details of the prepreg and the cure cycle for the glass adherend used for this experimental study is as given below in Table 2.

TABLE 2

GLASS/EPOXY ADHEREND LAYUP SEQUENCE

MATERIAL	LAYUP SEQUENCE	NOMINAL THICKNESS
GLASS/EPOXY FABRIC	$[0/45/90/-45]_S$	0.09175

The cure cycle for glass adherend is as follows:

- Heat the part to 270±10° F at a rate of 6° F per minute based upon the part thermocouple reading. The part must reach 270±10° F in 60 to 180 minutes.
- Hold at 270±10° F for 100±10 minutes. The hold period begins when the lowest part thermocouple reaches 260° F.

- Cool the part to below 170°F at a rate of 5° F per minute as measured on the part thermocouple while maintaining full vacuum.

Figure 2 illustrates the cure cycle for glass/epoxy adherend used for the experimental study.

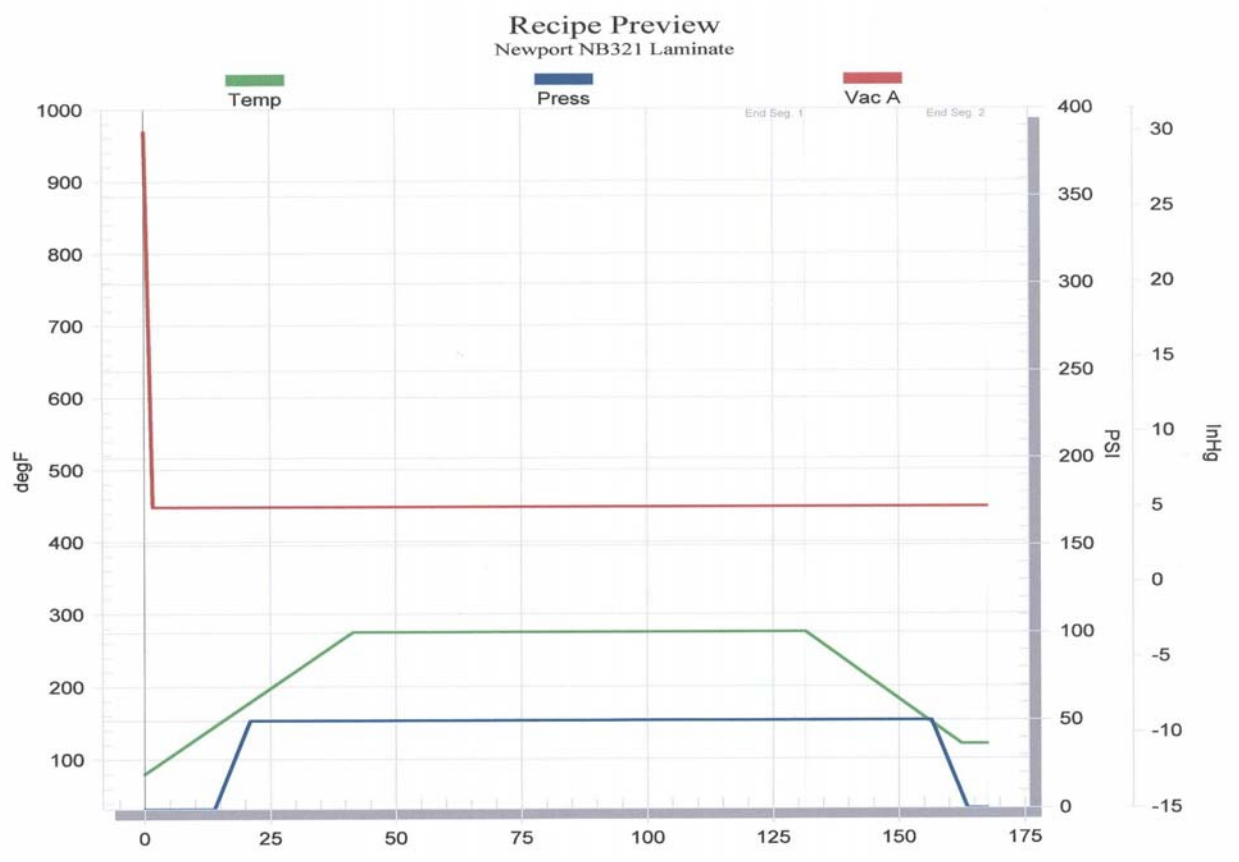

Figure 2. Cure cycle for glass/epoxy adherend.

3.1.2 Carbon Unitape Adherend

Carbon unitape adherend used for the experimental study was Toray T800S-3900-2B.

Layup details of the prepreg and the cure cycle for the carbon/epoxy unidirectional tape adherend for this experimental study is as given below in Table 3.

TABLE 3

CARBON/EPOXY UNIDIRECTIONAL TAPE ADHEREND LAYUP SEQUENCE

MATERIAL	LAYUP SEQUENCE	NOMINAL THICKNESS
CARBON/EPOXY UNIDIRECTIONAL TAPE	$[0/45/90/-45]_S$	0.0655

The cure cycle for carbon plain weave adherend is as follows:

- Apply the temperature ramp from ambient to 270 ± 10 °F at a rate of 3.0 ± 1.0°F per minute.
- Maintain the cure temperature at 270 ± 10 °F for 120 ~ 150 minutes.
- Cool down the temperature to 170 °F or lower at a rate of 4.5 ± 0.5 °F per minute before removing the vacuum.

Figure 3 illustrates the cure cycle for carbon/epoxy unidirectional adherend used for the experimental study.

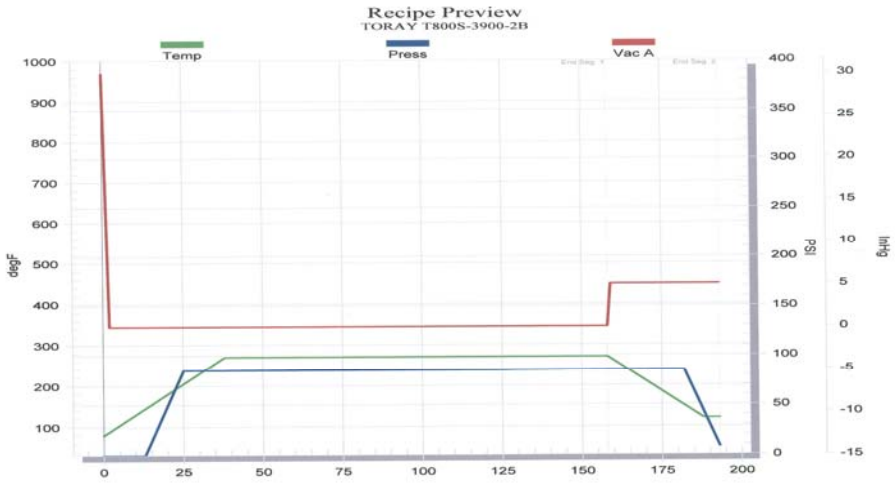

Figure 3. Cure cycle for carbon/epoxy unidirectional adherend.

3.1.3 Carbon/Epoxy Plain Weave Adherend

Carbon/epoxy plain weave adherend used for the experiment study is T700SC-12K-50C/#2510, which is a high strength standard modulus fiber with excellent processing characteristics.

Layup details of the prepreg and the cure cycle for the carbon/epoxy plain weave fabric adherend for this experimental study is as given below in Table 4.

TABLE 4

CARBON/EPOXY PLAIN WEAVE FABRIC ADHEREND LAYUP SEQUENCE

MATERIAL	LAYUP SEQUENCE	NOMINAL THICKNESS
CARBON/EPOXY PLAIN WEAVE FABRIC	$[0/45/90/-45]_S$	0.06795

The cure cycle for carbon/epoxy plain weave adherend is as follows:

- Apply the temperature ramp from ambient to 270 ± 10 °F at a rate of 3.0 ± 1.0°F per minute.
- Maintain the cure temperature at 270 ± 10 °F for 120 ~ 150 minutes.
- Cool down the temperature to 170 °F or lower at a rate of 4.5 ± 0.5 °F per minute before removing vacuum

Figure 4 illustrates the cure cycle for carbon/epoxy plain weave fabric adherend used for the experimental study.

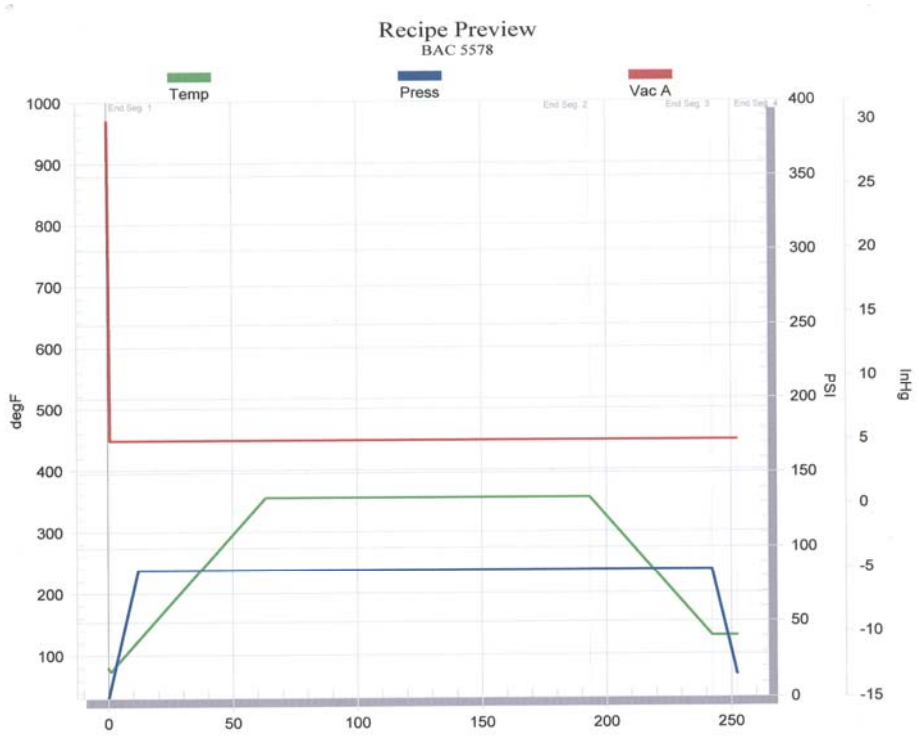

Figure 4. Cure cycle for carbon/epoxy plain weave fabric adherend.

3.1.4 Adhesive Selection

Adhesive selection was based on industry standards. Hysol EA 9394, which is a product of Henkel Corporation, widely used by aviation industry, was used for bonding of composite laminates. The selected adhesive is a two part structural adhesive which cures at room temperature and possesses excellent strength to 350°F/177°C and higher. Its thixotropic nature and excellent high temperature compressive strength also make it ideal for potting, filling and liquid shim applications. Besides these properties, this adhesive has long pot life, low toxicity and good gap filling capabilities which makes it a suitable adhesive for the research work which was carried on.

After selecting the right adhesive for bonding purpose, next step in specimen fabrication is to determine bondline thickness for the joint as well as the bonding method. Bondline

thickness selected for the purpose was 0.007".Such a thinner bondline thickness was selected because it was observed from references as well as from many trial runs conducted that thinner the bondline thickness is more the joint strength. Superior strength of the joint with a thinner bondline thickness is mainly due to the probability to have lesser chance of void formation in between the adherends and the adhesive layer.

Bonding was done by applying pressure on the adherends using clamps for fabrication of the joint. Hysol EA 9394 was applied on the trimmed composite panels as per instructed by the manufacturer. Adhesive is applied on one of the adherends to the specified bondline thickness and the other adherend is wetted using the same adhesive. The clamped specimens were then taken into an oven for curing. Accelerated curing was employed for bonding. As per the adhesive manufacturer, Hysol EA 9394 can be either cured for 3 to 5 days at 77°F or can be cured for 1hour at 150°F to achieve normal performance

The bonding procedure is as follows:

- Adherends were covered with utility tapes leaving the bonding area
- Part A and Part B of the adhesive were mixed at 100% to 17% ratio and stirred vigorously
- Spacers of thickness 0.007" were bonded to adherends using M-Bond 200 adhesive to control thickness of adhesive layer.
- Mixed paste adhesive is applied on one of the adherends and the other adherend is wetted using the same adhesive to control formation of voids , thus ensuring formation of an effective joint.

- The adherends are then placed on aluminum plates and clamped using C clamps manually
- After clamping, the adherends are taken to oven for curing.

The cure cycle for Hysol EA 9394 is as follows:

- Ramp up to 160°F from room temperature at a rate of 5°F per minute in 15 minutes
- After reaching 160°F in 15 min, the temperature is maintained for 60 mintues
- After 60 minutes, it is again cooled down to room temperature at a rate of 5°F per minute in 15 minutes

3.2 Panel Fabrication

While manufacturing a component using metals, it can be said that we start with the material in its final form even though some heat treatment processes may be essential to improve the properties of those metals. But when it comes to composite materials, they are made at the same time as the structure. Composite laminates for specimen fabrication for the experimental study was manufactured using vacuum bagging procedure and cured in an autoclave.

Vacuum bagging procedure is universal for any kind of structure. Prepregs are laid on a tool which usually made of aluminum. Before laying up the prepregs which form the laminate later on after curing, the tool is coated with a release agent. After coating with release agent, peel ply is laid on the tool. Peel plies are a tightly woven fabric, often nylon, and impregnated with some type of release agent. Peel plies often gives the texture for the composite laminate. Usually peel ply with rough finish is used as it helps in obtaining a better bonding while adhesives are used for bonding purpose. Next step in vacuum bagging is to apply a bag sealant tape along the sides of the tool. Bag sealant tape is a putty-like material which comes in rolls, usually 1/2 inch

wide, with a release paper on one side. After peel ply is laid on the tool, prepregs are stacked up in the correct stack up sequence. After stacking up the prepregs a caul sheet covered with peel ply is placed on top of the prepregs. On top of the caul sheet, a layer of breather cloth is placed. Breather is a thick, felt-like cloth which helps to absorb excess resin. It also provides a continuous air path for pulling the vacuum. Last step in completing the whole vacuum bagging procedure is the placing the bag. Vacuum bag material is a relatively thick plastic layer. The bag is usually applied along one edge at a time. Start at one corner and press the bag into the bag sealant tape, removing the release paper from the tape as you move along the edge. Before covering the tool with vacuum bag material, vacuum ports are attached. Usually base of the vacuum ports are placed on top of the breather cloth inside the vacuum bag and the attachment flange cuts comes out of the vacuum through a hole cut through the vacuum bag material. Vacuum ports are placed with utmost care so that there are not leaks on the sides of the port. Prepregs which are laid using this procedure are then taken to an autoclave and cured under required pressure and temperature conditions as directed by the composite manufacturer. Figure 5 shows the schematic representation of vacuum bagging stackup sequence.

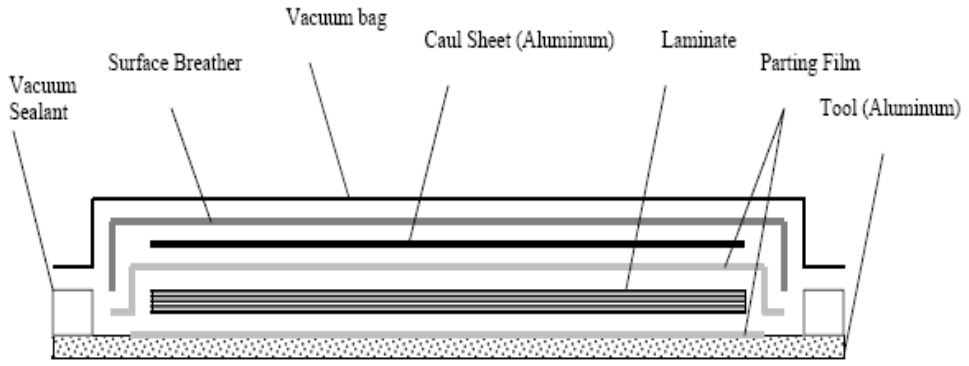

Figure 5. Vacuum bagging stack-up sequence.

3.3 Surface Preparation

Surface preparation plays a very vital role in adhesive bonding as pre-treatment of the surfaces to be bonded for forming a adhesive joint is crucial in establishing control over the quality and the effectiveness of the bond produced. Adhesive bonding depends on the establishment of intermolecular forces between the adherent and adhesive. Proper surface treatment ensures good bonding between the adherends and eventually integrity of the structure. The main objectives of surface preparation are as given below:

- to remove contamination
- to increase the polarity of the surface
- to increase the surface energy
- to increase the surface area
- to improve surface roughness
- to remove weak boundary layers

In this research, surface preparation of the specimen surfaces which are to be adhesively bonded was done as per standards which are prevalent in aviation industry and also matching with the adhesive manufacturer's specifications Sanding the surfaces can be done by two methods – either by using a sand blaster machine or by hand sanding. By using sand blaster machines under the correct pressure and feed rate can give a fairly even surface roughness. Hand sanding is also used for surface preparation. Specimen surfaces are roughened using specific grade of sand paper. But this method is not usually employed as this method gives surfaces of uneven roughness as compared to using sand blaster machines.

Hand sanding is used for surface preparation because of the specimen dimension. Sandblaster machines have a tendency to take off more material from the specimen surface than desired which is not desirable for this research. Composite panels are manufactured in autoclave to 18 inch by 18 inch in dimension out of glass fiber and carbon fiber prepregs. These cured composite panels are then trimmed to 17 inch by 17 inch in dimension for maintaining the perpendicularity as well as parallelism of the specimens and also to remove the extra resin which gets deposited on the sides during curing. These trimmed panels were then again milled down to two panels of dimension 6 inch by 17 inch as shown in Figure 7. The specimen surfaces were at first degreased using acetone. After drying off the acetone, the surfaces are roughened using a sand paper of grade 220 and after that those surfaces were subjected to water break testing. The roughened surface has to pass through water break testing. Water break testing is a means to check for discontinuity in the specimen surfaces which are sanded. If there is any discontinuity in the flow of water over the sanded surface, the specimens does not pass the water break test. If such discontinuities are present, those surfaces are to be cleaned with acetone and then roughened using sandpaper of the same grade until a continuous water flow is obtained which indicates that the specimen roughness is even all over the surface and it is ready for bonding.

3.4 Test Coupon Geometry

Composite laminates were bonded together to form a single lap joint. Lap joint was considered as the most suitable joint for this experimental study because of the ease of fabrication as well as the effectiveness to simulate an impact event occurring at joints in aircraft structures. Lap joint is one of the most commonly occurring joints and is the configuration often employed for adhesive testing.

Adherend dimensions were determined in accordance with ASTM D7136 standard. ASTM D7136 describes the test method for measuring the damage resistance of a fiber reinforced polymer matrix composite to a drop weight impact event. As described in the above said standard, adherend size for the test coupon was 4" × 6". Currently there is no specific standard available which says about the test coupon configuration for impact testing of an adhesively bonded lap joint, it was decided to follow ASTM D7136 to determine the adherend dimensions and overlap area for the lap joint was set to 3".Brass spaces of 0.007" were used during fabrication process of the test coupons to control bond line thickness. Figure 6. shows the specimen geometry and dimensions of the test coupons used for impact testing.

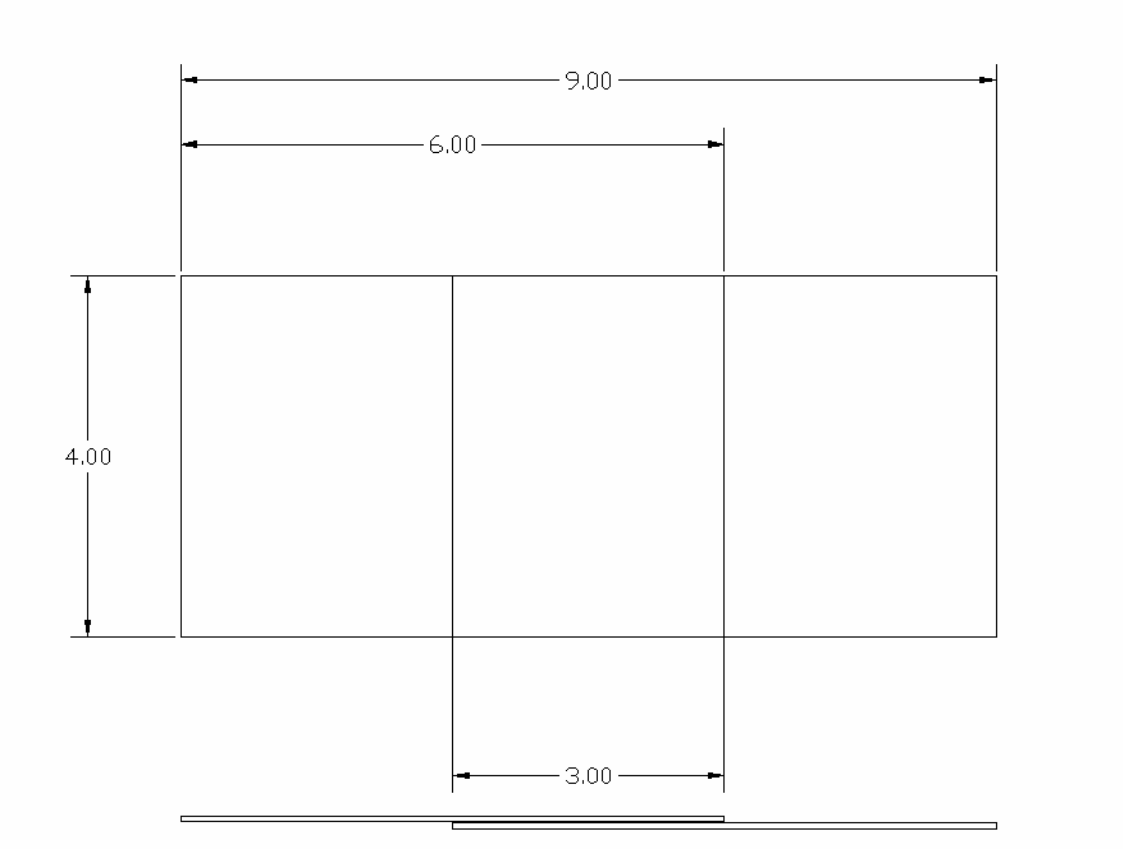

Figure 6. Test Coupon Geometry.

3.5 Test Coupon Fabrication

Composite panels which were trimmed down to 17" × 6" using a milling machine which uses a diamond coated blade was used for manufacture test coupons of dimensions 4"×6". Figure 7a. illustrates the panel trimming operation done on the adherend panels used for the experimental study. After roughening the bond area on panels of above said dimension, brass spaces of thickness 0.007" were placed on locations as shown in Figure 7b. Hysol EA 9394 is mixed as per manufacturer specifications and is uniformly spread over the overlap area. Adherends are then clamped down together using C-clamps and taken to an over for curing as per adhesive cure cycle mentioned earlier in this section. After curing, those panels are machined to test coupon dimensions as mentioned above.

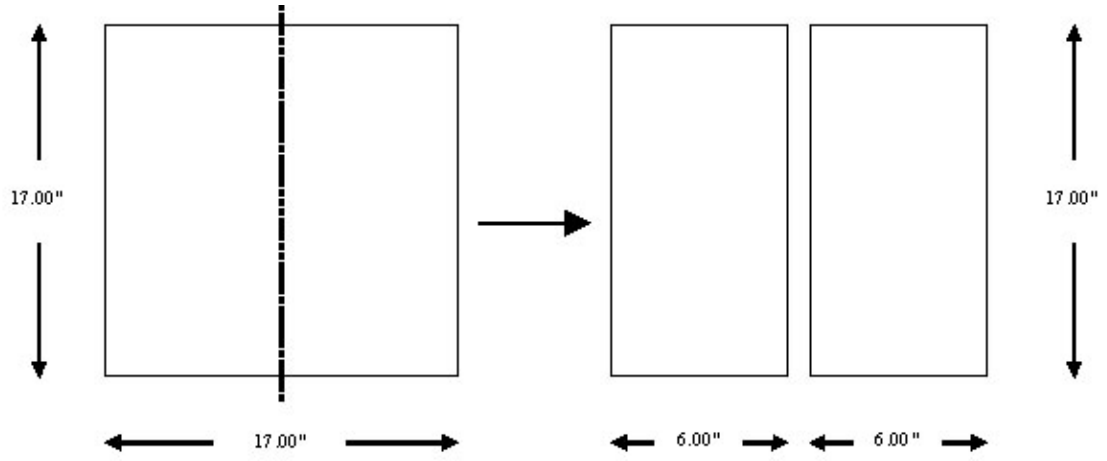

Figure 7a. Panel Trimming Operation.

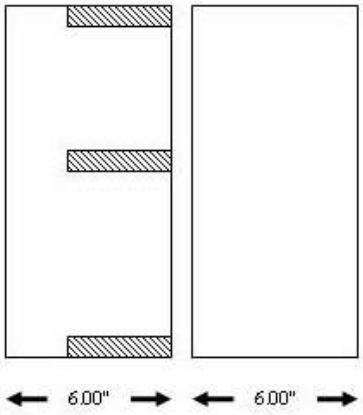

Figure 7b. Brass spacer position used for bonding adherend panels.

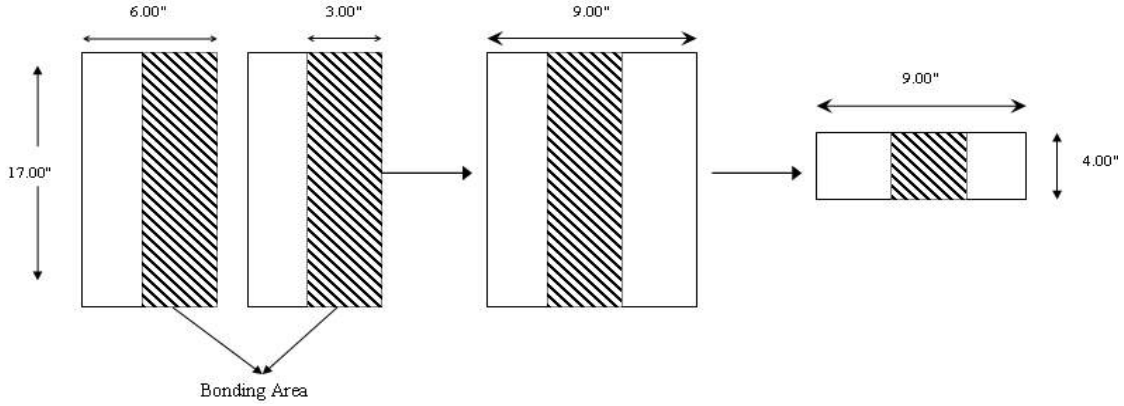

Figure 8. Test coupon fabrication process.

CHAPTER 4

TEST MATRIX AND SPECIMEN NOMENCLATURE

4.1 Test Matrix

Data points required for generating force displacement curves, impact force history and total energy history were obtained from impact testing done on the test coupons using an Instron Dynatup 8250 drop weight tester. Table 5 shows the test matrix for experimental study. Adherends made up of three material systems were used for the experimental study. The test coupons were impacted using impactors of three different impactor diameters. The test coupons were impacted at different energy levels for each impactor diameter.

TABLE 5

TEST MATRIX FOR IMPACT TESTING

MATERIAL	IMPACTOR DIAMETER [in]	ENERGY LEVEL [J]	NO:OF SPECIMENS
NEWPORT NB321	0.50	10	2
		25	3
		40	3
	0.75	10	2
		25	3
		40	3
	1.00	10	2
		25	3
		40	3
TORAY T800SC UNITAPE	0.50	10	2
		25	3
		40	3
	0.75	10	2
		25	3
		40	3
	1.00	10	2
		25	3
		40	3
TORAY T700 12K PALIN WEAVE	0.50	10	2
		25	3
		40	3
	0.75	10	2
		25	3
		40	3
	1.00	10	2
		25	3
		40	3
		TOTAL NO: OF SPECIMENS	72

4.2 Specimen Nomenclature

Impact testing was done on a total of 72 test coupons. Because of the vast number of coupons to be tested for the experimental study a common naming nomenclature was employed for identifying the specimens. All the test coupons were named based on the nomenclature as shown in Table 6.

TABLE 6

SPECIMEN NOMENCLATURE

Event	Adhesive	Adherend	Panel#	Impactor Dia	Energy Level	Specimen #
I Impact	1 EA 9394	G NEWPORT NB321	1	1 1"	A 10	1 Specimen 1
		U TORAY T800SC	2	2 0.75"	B 25	2 Specimen 2
		P TORAY T700 12K	3	3 0.5"	C 40	3 Specimen 3
			4			
			5			
			6			
			7			
			8			
			9			

CHAPTER 5

IMPACT TESTING

Impact loading was done on the adhesively jointed composite coupons for the experimental study using a Instron Dynatup 8250 Drop Weight Impact Tester. This machine is equipped with a pneumatic rebound catch mechanism and data acquisition software which runs on a computer connected to the drop weight impact tester. Data from Instron Dynatup 8250 Drop Weight Impact Tester is acquired with Instron Dynatup Model 930-I data acquisition system. This following section describes mainly about the impact testing machine and the impact testing procedure.

5.1 General Description

Instron Dynatup 8250 Drop Tower consists of the following features:

- Two guide columns
- Hoist motor
- Drop-weight mechanism
- Control pendant
- A pneumatic rebound-catch mechanism which prevents secondary impacts on the test coupon
- A photo-detector/flag system which provides impact velocity information

5.1.1 Specifications

The following specifications apply to Instron Dynatup 8250 Drop Weight Tester

- Impactor Weight

  Minimum Weight: 3.60 lbs

  Maximum Weight: 26.05 lbs

- Impactor Diameter

  Hemispherical 0.5″, 0.625″, 0.75″ and 1.0″

- Impact Energy

  Impact energies ranging from 0.67 J – 302 J

- Impact Velocity

  Impact velocity ranging from 1,440 in/min – 9,144 in/min

- Drop Height

  Maximum of 40″

- Load Cell

  Type: Piezoelectric

  Capacity: 0-5000 lbf

- Rebound – Catch Mechanism

  Optimum detectable rebound height: 1″

- Data Acquisiton

Signal Source: Tup

Sampling Frequency Range: 82 kHz – 2.05 MHz

Filter: 4 kHz

Trigger: External (photoelectric)

- Fixtures

  Test fixtures available with test section of 5" × 3" and 5" × 5"

- Air Requirements

  Pressure: 85-95 psi

This drop tower consists of two long guide columns that are held in alignment and are fixed between the base plate and the fixed top cross head. The guide columns are made up of stainless steel and are of 1" in diameter. Drop weight assembly which is is the main component of this machine moves up and down through these guide columns. Drop weight assembly consists of a drop weight mechanism, which comprises of a release mechanism, an upper cross member and a lower cross member. Upper cross member is attached to the dropweight assembly by means of a hook. It is in between the upper and lower cross members add on weights are attached to obtain various impactor weights. Load cell as well as the tup is attached to the drop weight assembly through the lower cross member by means of a long screw. Tups are usually hemispherical in shape and are made up of hardened steel. The base plate of the machine is provided with a hole of diameter 4". Test coupons which are to be impacted are placed on a fixture which is kept under the base plate of the machine. Different kinds of fixtures are available to hold coupons of different sizes under clamped boundary conditions. Two kinds of clamping fixtures are available for holding the test coupons depending on the test coupon sizes. Smaller

coupons could be placed on the test fixture shown in Figure 9. Figure 10 shows the test fixture for experimental study. Impactors used for the experimental study are shown in Figure 11. Figure 12 shows the experimental setup used for experimental study.

Figure 9. Test fixture for impacting small coupons.

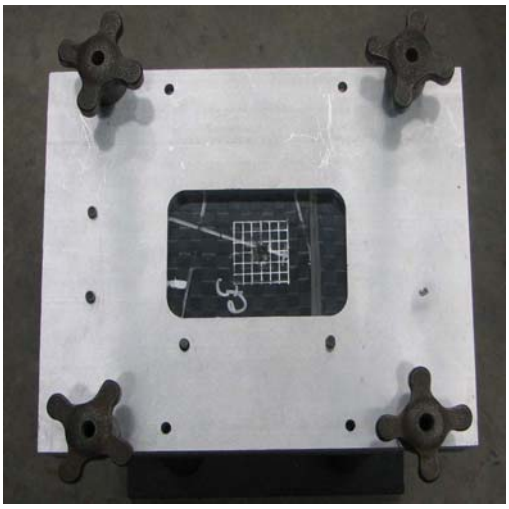

Figure 10. Test fixture for experimental study.

Figure 11. Impactors used for the experimental study.

This fixture is provided with dowel pins which makes helps in aligning the test coupon at the correct position. Clamps provided on this fixture are used to clamp down the test coupon

which prevents movement of the test coupon. Usually coupons of size 4" × 6" are impacted using this kind of test fixture. Another kind of test fixture available for impacting of the test coupons is shown in Figure 10. This fixture comprises of two aluminum or steel plates with each plate containing an opening in the middle which enables to impact the test section on that coupon.

Figure 12. Instron Dynatup Drop Weight Tester Used For Experimental Study.

One of these plates is provided with dowel pins which enable to align the test coupon at the correct position. These plates are clamped down to the test stand using four screws from the test stand at the four corners of the test fixture.

During an impact event, the impactor usually bounces due to the impact on the specimen. In order to prevent the impactor from inflicting secondary impacts on the specimen, a pneumatic rebound-catch mechanism is employed. Rebound catch mechanism for Instron Dynatup 8250 Drop Tower consists of a shock absorber and a stop block setup. Shock absorber setup consists of two air cylinders located close to the guide columns. The piston for those air cylinders are

activated by compressed air. The end of the piston which comes in contact with the dropweight assembly is made up of elastomeric material which helps to prevent damage for the dropweight assembly.

5.1.2 Data Acquisition

During an impact event, forces will be applied on the test coupon typically for an interval of 0 to 10 milliseconds as shown in Figure 13. All the required data which has to be extracted from the experiment has to be recorded in such a small time interval. For that purpose, a system which is capable of capturing the data effectively should be employed. Data acquisition should be done only during the time of impact in order to keep the amount of data to the minimum. In order to do that, an automatic triggering device should be also present in the test machine which initiates data acquisition at the right time.

Instron Dynatup 8250 Drop tower is equipped with Instron Dynatup Impulse data acquisition system which could be termed as the *heart* of the impact testing machine. Impulse data acquisition system is a combination of both hardware and software components. It comprises an instrumented tup, the Impulse data acquisition software, the Impulse signal conditioning unit (ISCU), and one of a range of National Instruments data acquisition cards. Among the hardware components which comprise the data acquisition setup of the test machine, photo-detector/flag system which provides impact velocity information plays a vital role and particular notice should be given to the role which it plays in the whole testing. Photo-detector/flag system which detects the velocity of impact comprises of a velocity detector flag which is mounted on the drop weight assembly and a velocity detector block mounted close to the path of the drop weight assembly. Velocity detector block incorporates a photo electric sensor which has an emitter and a receiver, in which the emitter produces a non-pulsating

infrared beam. The gap present in between the emitter and the receiver provides the path for the velocity detector flag which during the impact testing interrupts the infrared beam. As a result of this interruption of the infrared beam, a voltage pulse is produced. This voltage pulse is used to trigger the data acquisition as well as to measure the impact velocity.

For successful data acquisition, both hardware part and the software part should work in unison. Dynatup 8250 drop tower uses a computer program called Impulse, which is a very powerful as well as an user friendly program. This program allows inputting user defined tracking information, specimen information for each test coupon. This program displays a wide variety of acquired signals in a single window and also allows importing and exporting the data into an user-specified file. A screen display of the program in shown in Figure 13.

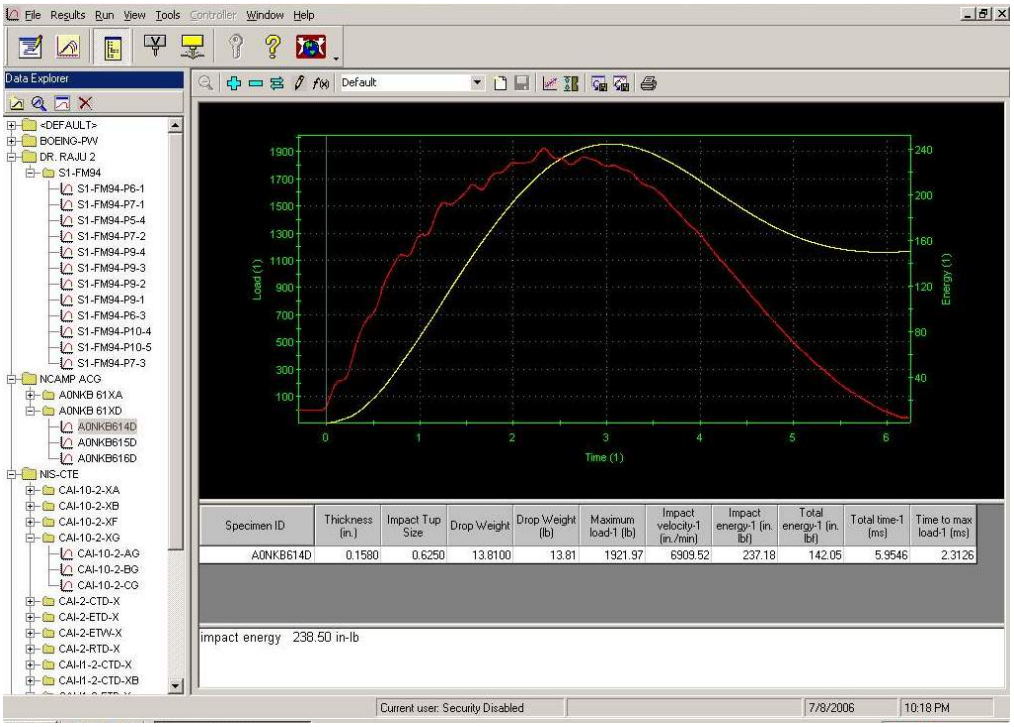

Figure 13. Screen shot of Impulse data acquisition software.

Adhesively bonded composite joints were impacted at the center of the overlap region using Instron Dynatup 8250 Drop Weight Tester which was described in detail in the above

section. The test coupons were impacted over a range of impact energies as well as using impactors of varying diameters. The range of impact energies used for the experimental study was from 10J to 40 J and the diameter range of the impactors were from 0.5″ to 1.0″. Data reported from an impact test are force time history, displacement time history, velocity time history and energy time history. The following section describes basic procedure for impact testing.

5.2 Setting up Velocity Detector Block

Before performing an impact test, velocity detector has to be positioned at the correct height. If the velocity detector block is not positioned at the right position, all the data acquired from the impact test will not be accurate. The following steps have to be followed while setting up the velocity detector.

1. Place the specimen on the desired support fixture
2. Lower the crosshead until the tup rests on the specimen
3. Loosen the two screws that attach the velocity detector to its support bracket
4. Slide the velocity detector up or down until the edge of interest of the velocity detector flag is approximately 0.25″ below the center line of the velocity detector.
5. Check that the flag passes through the center of the velocity detector slot
6. Secure the velocity detector to the support bracket

5.3 Running a Velocity Test

After setting up velocity detector block successfully, a velocity test has to be conducted. Velocity test is conducted for the following reasons:

- Establish a height for the drop weight that will give the required velocity
- To find out what velocity is being achieved at the current drop height.
- Confirm that the value that you have set as the target velocity for the dropweight is actually being achieved.

Below given procedure has to be followed while running a velocity test:

a. From the menu bar in the Impulse data acquisition software, click on Run Velocity Test button.

b. Using the control pendant, position the drop weight to the required height

c. No specimen should be installed in the support fixtures

d. Make sure the rebound – catch mechanism is turned on

e. When ready to run the velocity test, press *fire* button in the control pendant

f. A window will pop up after the velocity test which indicates the impact velocity

Impact velocity could be determined analytically using the following equation:

$$v = \sqrt{2gh} \qquad \textbf{(5. 1)}$$

where v = theoretical velocity in in/min

g = acceleration due to gravity in in/min^2

h = drop height in inches

5.4 Running an Impact Test

a. From the menu bar in the Impulse data acquisition software, click on Run Impact Test button. A window pops up which is used to specify the method used for impact testing.

b. After inputting all the required information in above said window, when Next is clicked, another window opens up where all the test coupon tracking information is entered and in the following window all the test coupon information has to be entered.

c. After inputting all these preliminary information, specimen is placed on the support fixtures

d. By hitting **Next**, machine is ready to run impact test.

e. Using control pendant, the drop weight is made to fall under gravity by pressing the fire button.

f. After impacting is done, software generates force time graphs and energy time graphs.

CHAPTER 6

NON-DESTRUCTIVE TESTING

Non-destructive testing is now an essential part of quality assurance, to determine the quality or integrity of an item non – destructively, find a physical phenomenon that will interact with and be influenced by the test specimen without altering the specimen's function. Damage due to an impact event may be cracking of the matrix, fiber breakage, debonding which occurs internally within the specimen. Matrix cracking as well as fiber breakage can be quantified visually but debonding cannot be quantified using visual inspection. In order to assess damage caused due to debonding, non destructive testing using through transmission ultrasonic C-scan inspection is carried out. In this experimental study, SDI 5000 Series Ultrasonic system is used for C-scan inspection of the impacted test coupons. The following section describes about the details of the equipment used for non-destructive inspection as well as the through transmission ultrasonic C-scanning procedure followed for non destructive inspection of impacted test coupons. This chapter also discusses briefly about the residual indentation measurement procedure.

6.1 General Description

SDI 5000 Series Ultrasonic system which is an ultrasonic immersion inspection system is being used for a wide variety of applications. An ultrasonic system is said to be comprised of three main components:

- Mechanical Scanner Mechanism
- Motion Control Hardware and Software
- Flaw Detector

- Data acquisition hardware and software

A typical ultrasonic inspection system is shown in Figure 14.

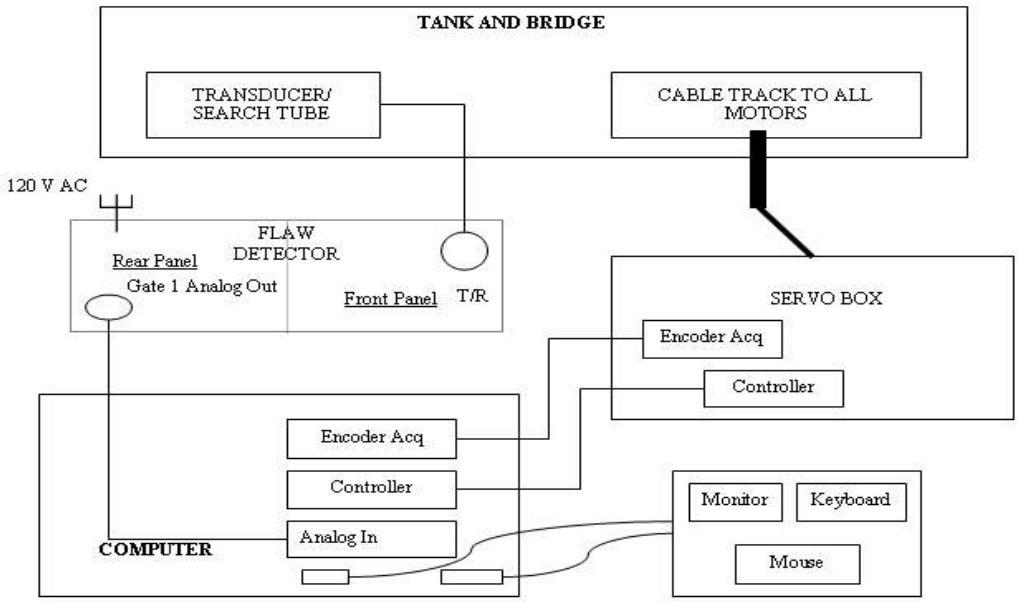

Figure 14. Schematic Representation of Ultrasonic Inspection System.

Above said components were the three main categories in which the components of an ultrasonic system could be included. On a broader classification, such systems consist of the following components:

- Immersion tank
- Bridge (X,Y,Z axes)
- Gimballs (A,B)
- Servo box
- Recirculation pump, water filter and skimmer
- Computer

- Motion control software and hardware
- Ultrasonic transducers
- Flaw Detector
- Data acquisition software and hardware

6.2 Non-Destructive Testing Procedure

Through transmission ultrasonic C-scan method was used to obtain the planar damage of the impacted test coupons. This kind of non-destructive testing procedure involves transmission of ultrasonic waves across the specimen through transducers located on either side of the specimen and obtaining a planar damage pattern through differences in the signal attenuation levels. This equipment uses a method called *pitch-catch* method, in which the signal emitted by one transducer is transmitted to another one located on the other side of the specimen, which transforms this signal into an electrical pulse which with the help of MASTERSCAN software converts into a digital image of the damage induced in the test coupon. All the impacted test coupons were scanned along the X direction using flat 2 MHz transducers at a scan speed of 0.02 in/s along the length and with an index increment of 0.02 inches to get maximum resolution for the scanned image. Other than the index increment and scan speed, another factor which plays a vital role in wave 'gain' value. The scanned image, usually gray scale image is opened in SDI-WinScan Analysis, software used for computing damage area on the test coupon. Figure 15 shows the screenshot of SDI-WinScan Analysis window. A histogram analysis is done to find out damage area induced in the test coupon. The grayscale image obtained from C-scanning is quantized into percent levels, 1 percent levels and 256 percent levels which gives a better representation of what the A to D is doing. Lower percent levels indicate to color white

where as the higher percent level indicate color black. To find the damage area, a threshold value is selected. During image analysis, whatever shades comes below the threshold value is considered as damaged regions and whatever shades comes above the threshold value is considered as undamaged area. Thus the damage area is calculated by SDI-WinScan Analysis.

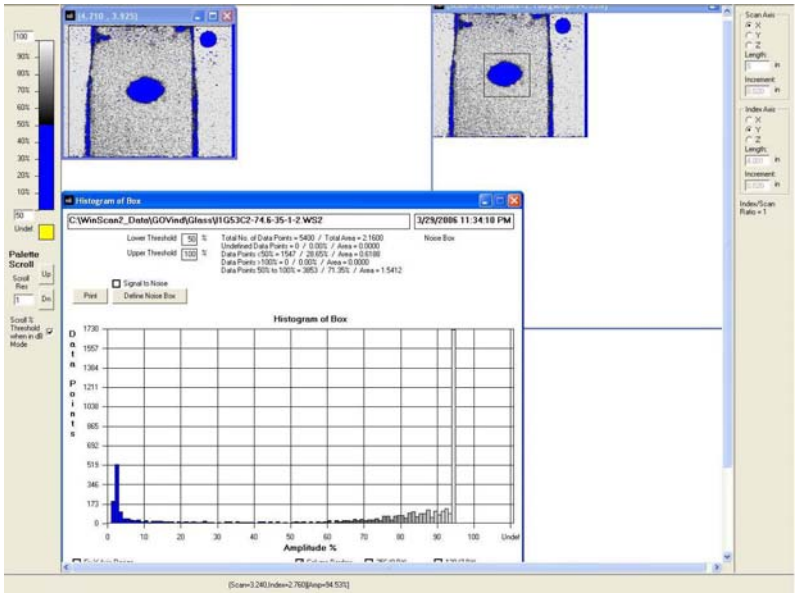

Figure 15. Screenshot of SDI-WinScan Analysis.

6.3 Residual Indentation Distribution

The impacted test coupons which were inspected using through transmission C-scan are then inspected again non – destructively for residual indentation distribution in the vicinity of impact point. The indentation produced due to impacting was measured using a digital indicator. Resolution of the digital indicator is 0.0005″ and has a range of ±1.0000″. The indentation is measured over an area of 1.50″ × 1.50″ with the center at the impact point, with a grid size of 0.25″ in both directions. Figure 16. shows the setup for the residual indentation depth measurement. Figure 17. shows the grid used for depth measurement. The residual indentation depth data for each specimen is recorded. Data obtained is then used to obtain surface plots.

Surface plots for impacted test coupons are generated using Golden Software's SURFER 8.0 computer program.

Figure 16. Setup for residual indentation depth measurement.

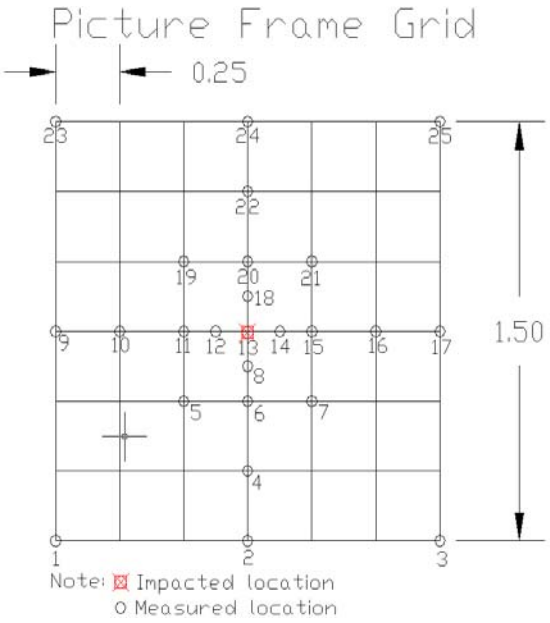

Figure 17. Depth measurement Grid.

CHAPTER 7

RESULTS AND DISCUSSIONS

7.1 Impact Test Results

Behavior of adhesively bonded composite joints to different impact energy level as well to different impactor diameters is discussed in the following section. Impact tests were done on test coupons fabricated from woven glass/epoxy, carbon/epoxy plain weave fabric and carbon/epoxy unitape adherends. All the test coupons were clamped down to the test fixture as shown in Figure 10 in the previous section, with a test section of 3″ × 5″. Parameters which were used to quantify the impact response of these test coupons were maximum impact force, total energy absorbed, duration of impact and impactor displacement.

Figure 18 to Figure 26 show the typical force displacement, impact force-time and energy time plots for test coupons impacted at 40J with impactors having impactor diameter 0.5″, 0.75″, 1.0″ respectively. Force-time history of the above said three materials with different impactor sizes are totally different. From the plots its evident that impactor with smaller diameter, 0.5″ induces more damage in the form of matrix cracking, fiber cracking which leads to penetration rather than compared with impactors with larger diameters. Impactors with larger impactor diameters induce more impact force on the test coupons primarily due to larger contact area at the point of contact. Due to the above said phenomena, the load which is applied on the test coupon gets distributed to a larger area which leads to larger internal damage. Typically, smaller diameter impactors induce damage in the form of fiber cracking; it has been observed that the internal damage area is comparatively lesser than the damage area produced by impacts due to impactors with larger diameters.

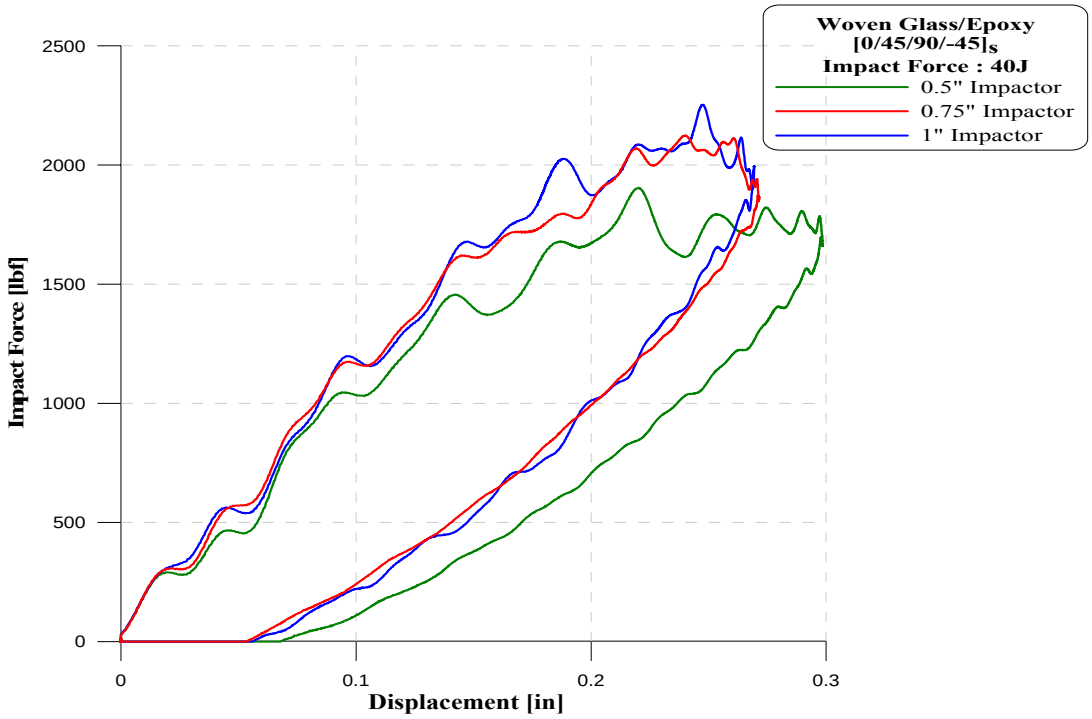

Figure 18. Typical Force – Displacement curves for woven glass/epoxy test coupons.

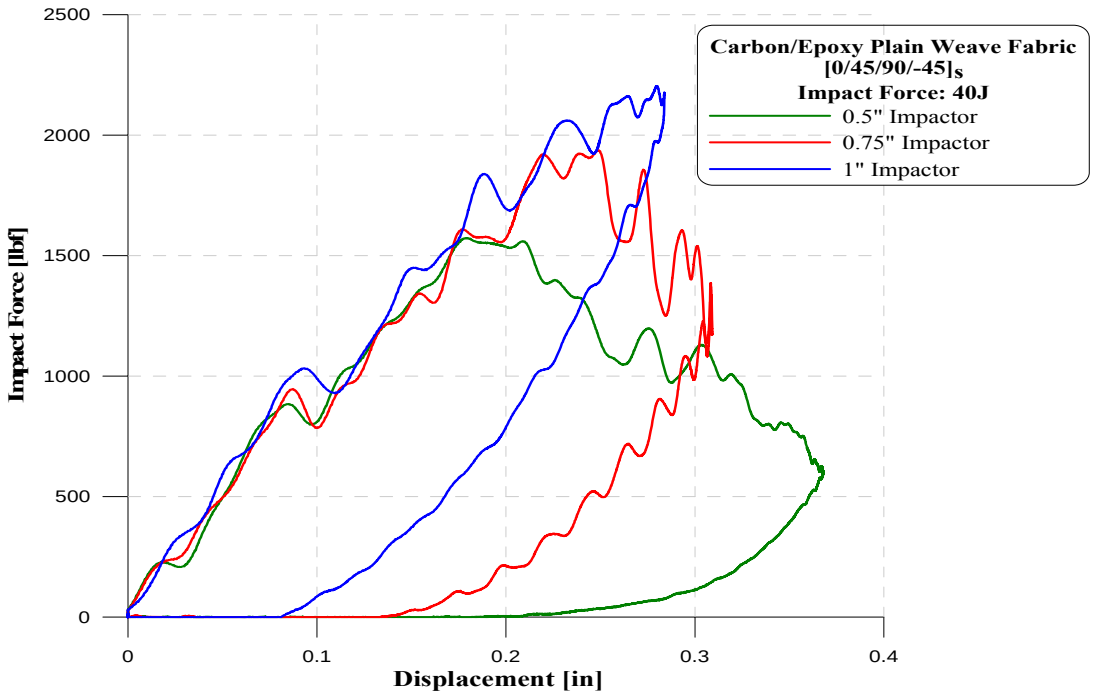

Figure 19. Typical Force – Displacement curves for carbon/epxoy plain weave fabric test coupons.

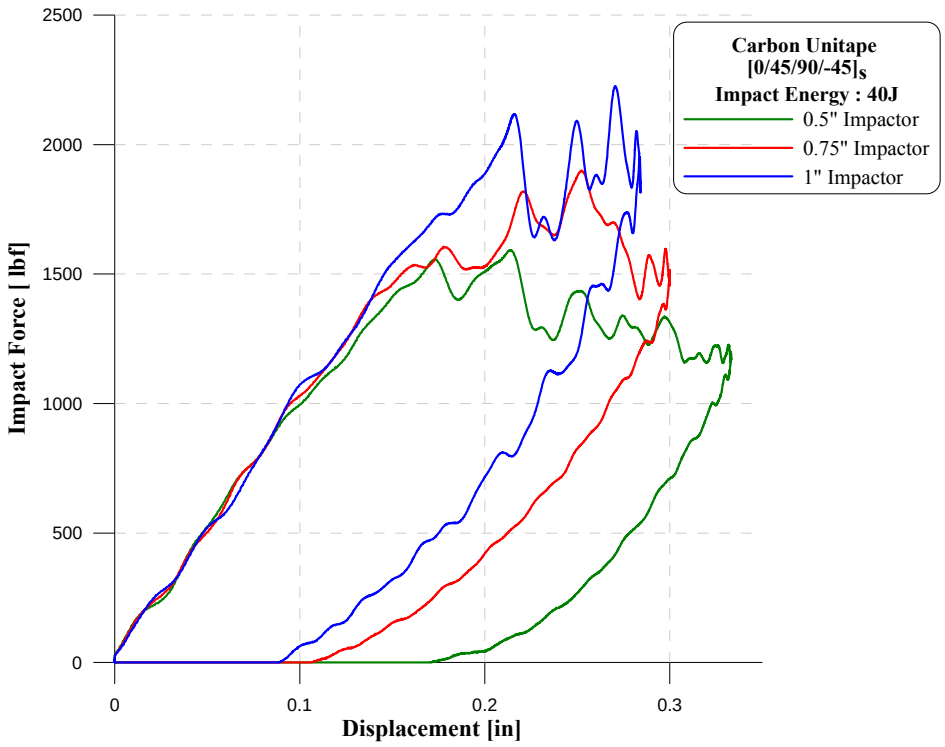

Figure 20. Typical Force – Displacement curves for carbon unitape test coupons.

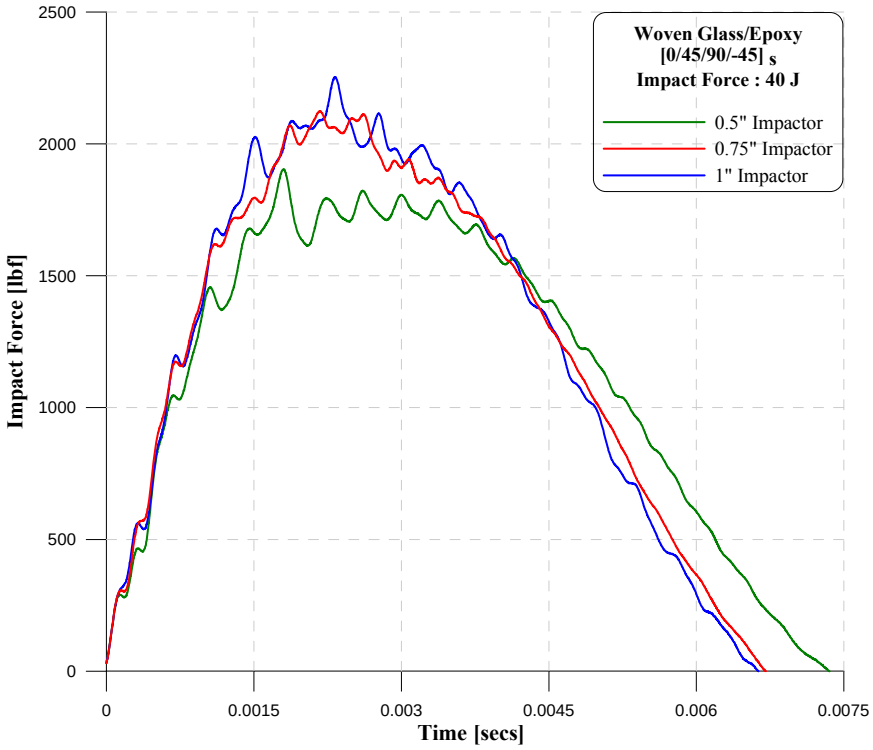

Figure 21. Typical Impact Force – Time curves for woven glass/epoxy test coupons.

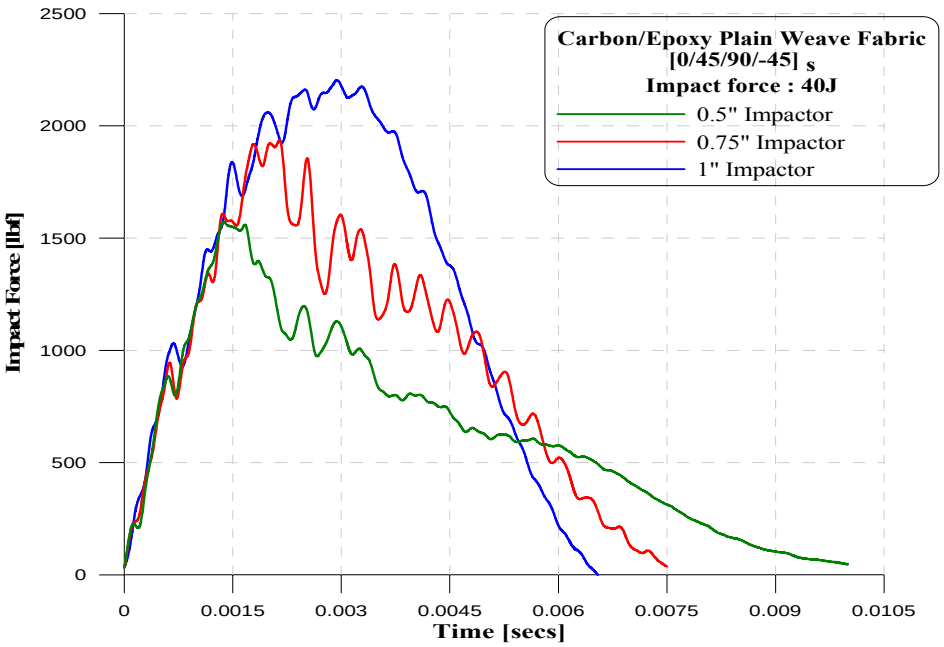

Figure 22. Typical Force – Displacement curves for carbon/epoxy plain weave fabric test coupons.

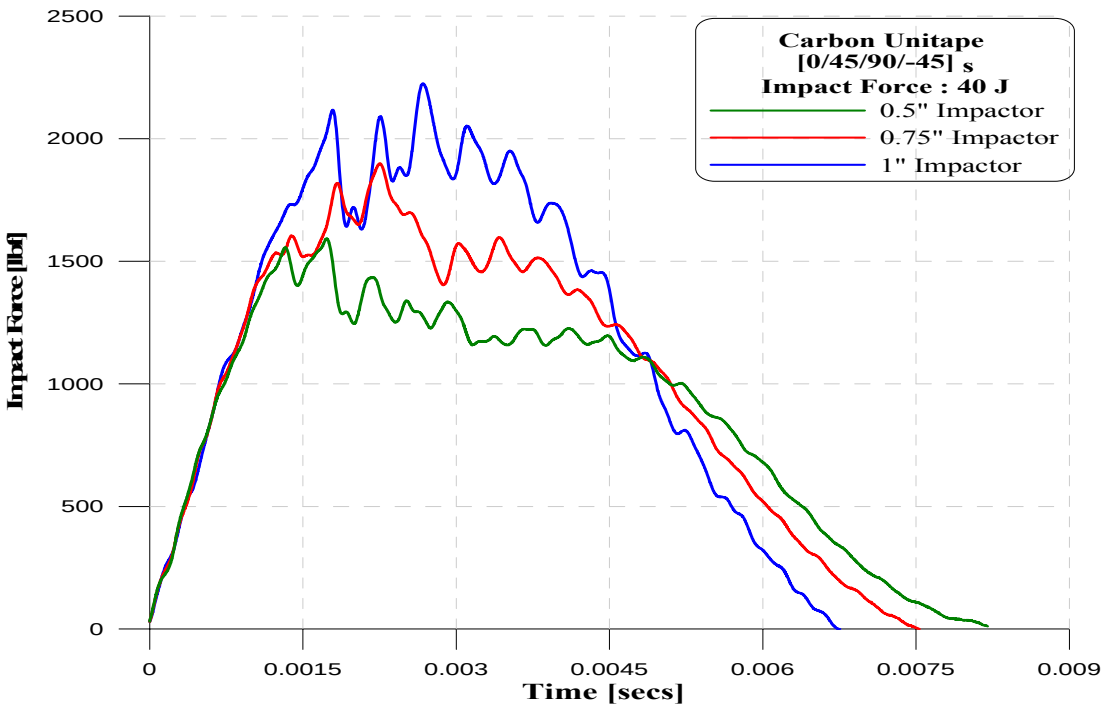

Figure 23. Typical Impact Force – Time curves for carbon unitape test coupons.

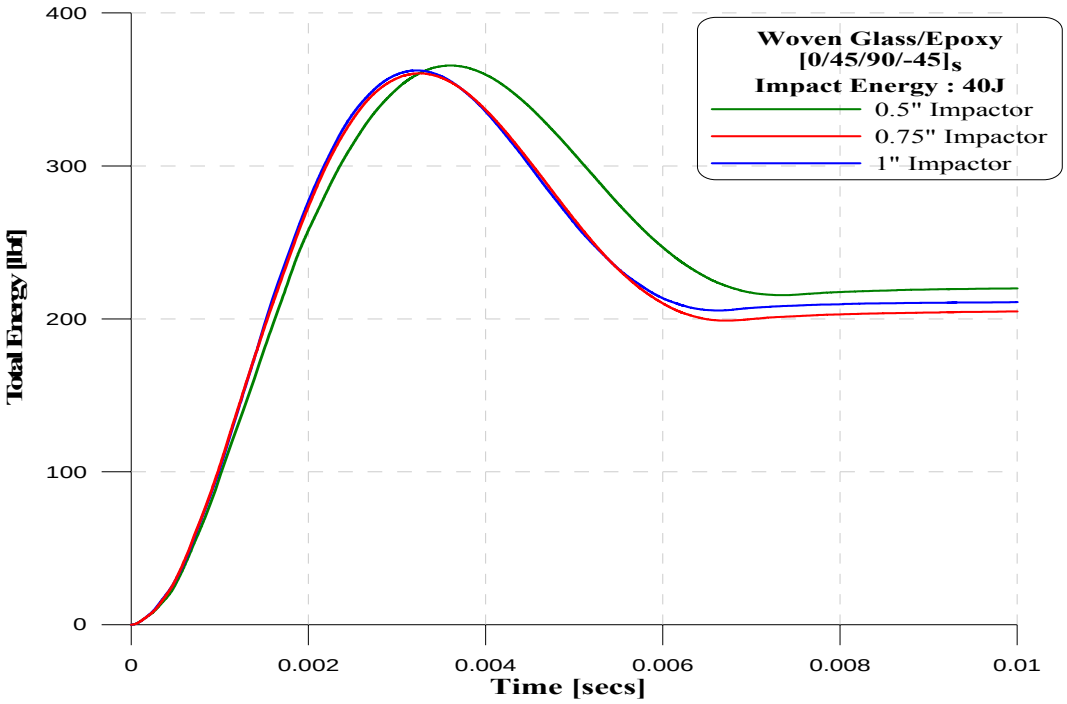

Figure 24. Typical Total Energy – Time curves for woven glass/epoxy test coupons.

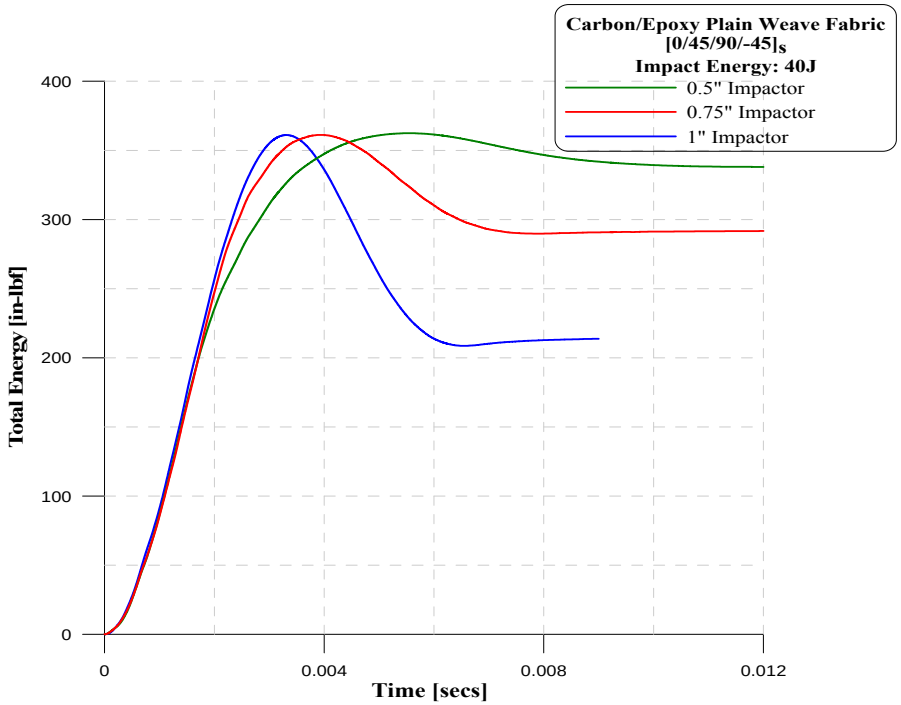

Figure 25. Typical Total Energy - Time curves for carbon/epoxy plain weave fabric test coupons.

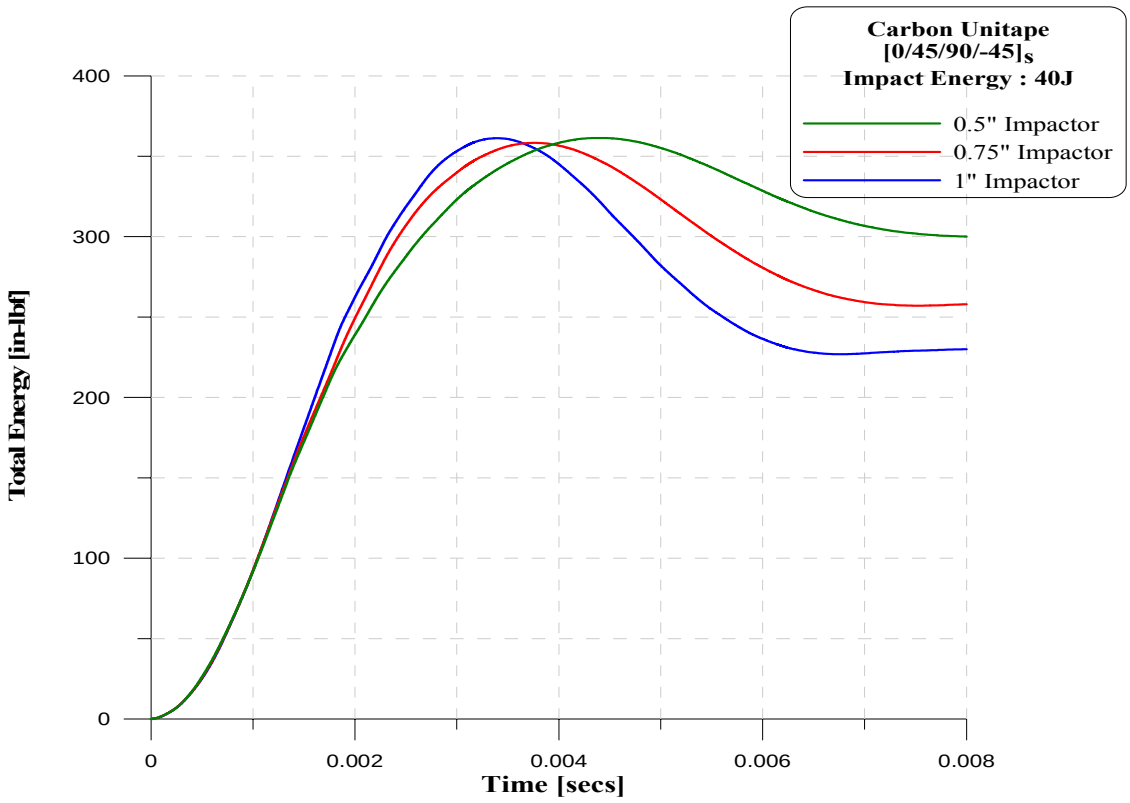

Figure 26. Typical Total Energy – Time curves for carbon unitape test coupons.

7.2 Non Destructive Test Results

Impact damaged specimens were subjected to through transmission ultrasonic C-scanning for mapping of debonded regions and to assess the damage area induced on the test coupons due to impact.

Figure 27 to Figure 35 show the images of the damage induced on woven glass/epoxy, carbon unitape and carbon plain weave specimens at 40J impact energy induced by impactors of diameters 0.5″, 0.75″, 1.0″ respectively.

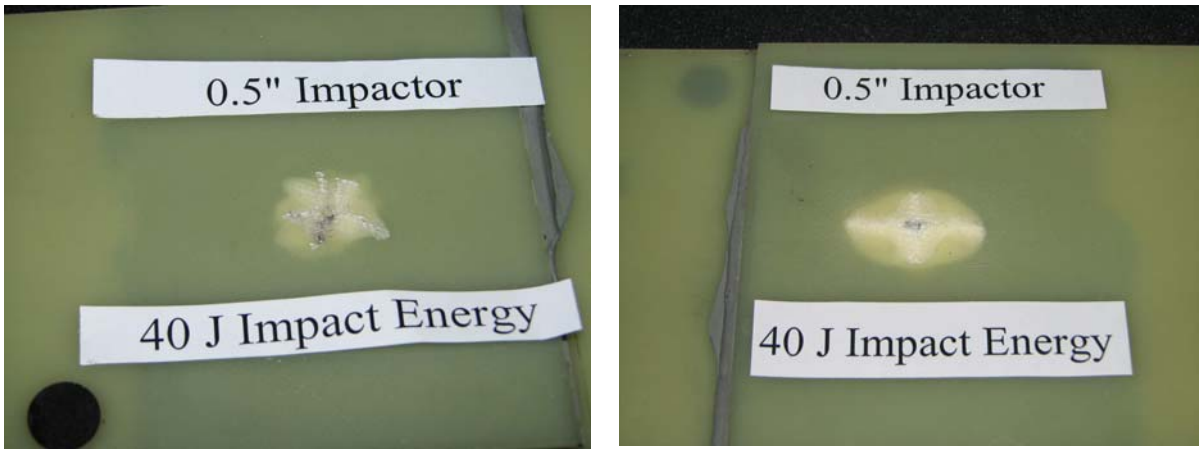

Figure 27. Damage induced on woven glass/epoxy test coupon impacted at 40J with 0.5" impactor

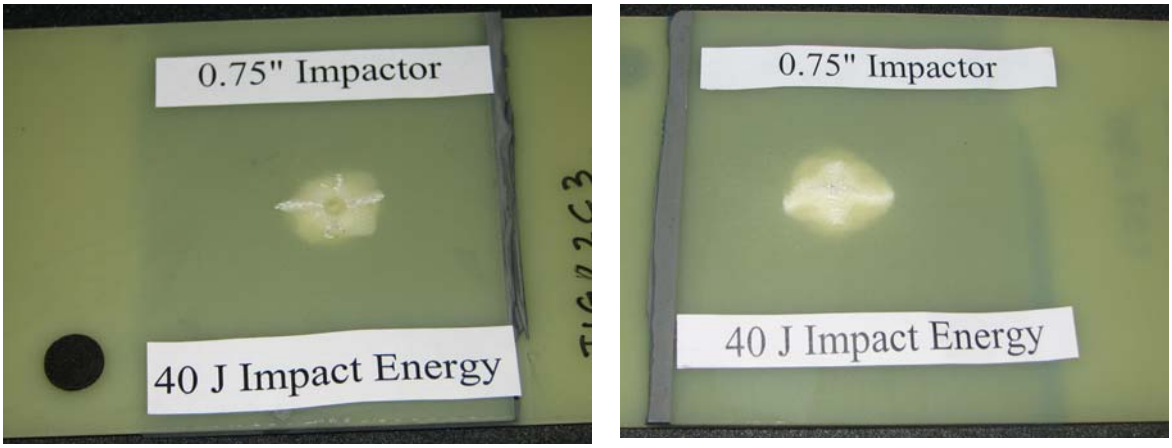

Figure 28. Damage induced on woven glass/epoxy test coupon impacted at 40J with 0.75" impactor

Figure 29. Damage induced on woven glass/epoxy test coupon impacted at 40J with 1.00" impactor.

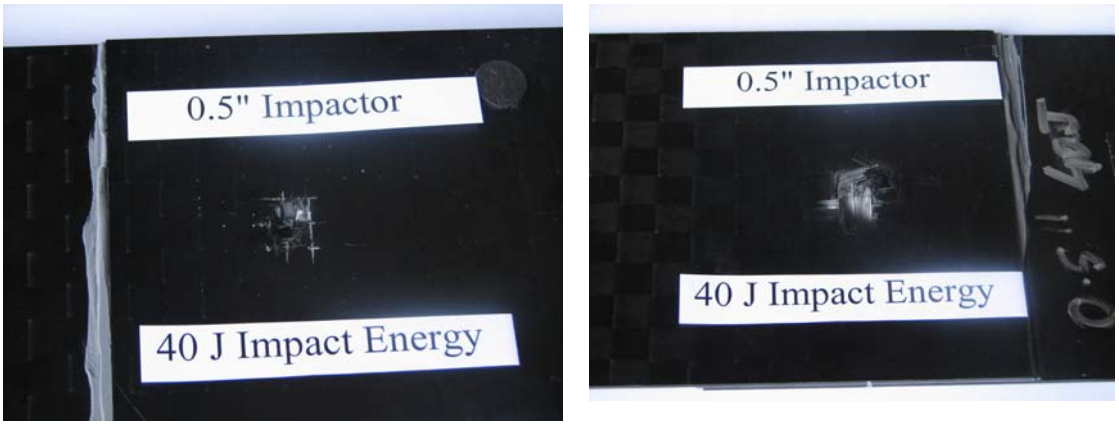

Figure 30. Damage induced on carbon plain weave/fabric test coupon impacted at 40J with 0.5" impactor.

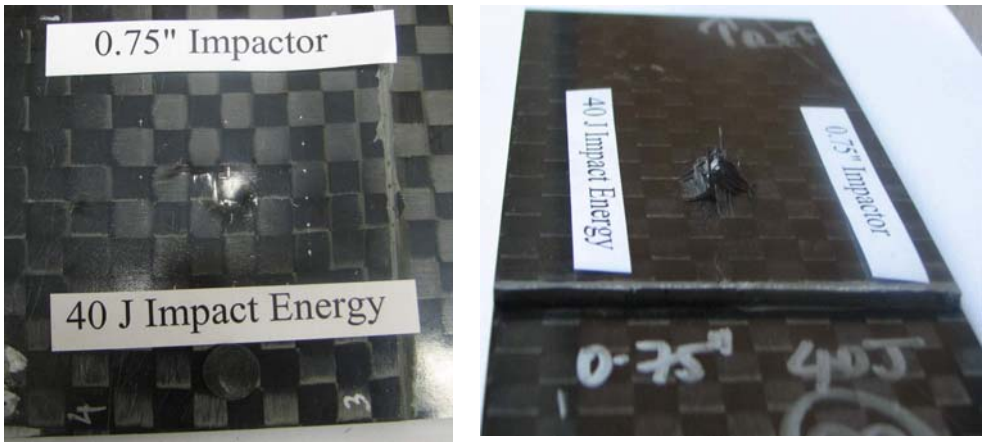

Figure 31. Damage induced on carbon plain weave/fabric test coupon impacted at 40J with 0.75" impactor.

Figure 32. Damage induced on carbon plain weave/fabric test coupon impacted at 40J with 1.00" impactor.

Figure 33. Damage induced on carbon unitape test coupon impacted at 40J with 0.5" impactor.

Figure 34. Damage induced on carbon unitape test coupon impacted at 40J with 0.75" impactor.

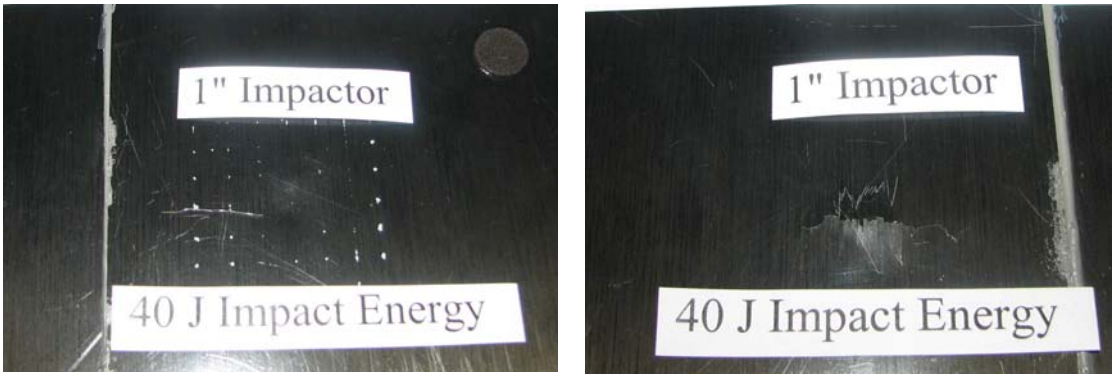

Figure 35. Damage induced on carbon unitape test coupon impacted at 40J with 1.00" impactor.

Figure 36 through Figure 38 show the through transmission ultrasonic C- scan images of the damage induced on woven glass/epoxy, carbon unitape and carbon plain weave specimens at 40J impact energy induced by impactors of diameters 0.5″, 0.75″, 1.0″ respectively.

Figure 39 through Figure 41 represents plots which show the relationship between damage area and impact energy. Damage process in composites take place as a result of matrix cracking which induce delamination in between ply interfaces. Matrix cracks are induced on the first layer at first because of high localized stresses. Further progression of the damage happens

from upper to the bottom layers. This progression follows a pattern which is called as pine tree pattern. More damage area is observed in carbon fiber adherends compared to glass fiber adherends. In glass fiber adherends, as the impactor diameter increases the damage area also increases linearly. While, in carbon plain weave adherends, damage area increases and reaches a maximum and then drop down with increase in energy level. This shows that in carbon plain weave material, damage area reaches a threshold value at specific impact energy level and after that propagation of damage does not take place as at higher energy levels with a specific impactor, instead formation of highly localized stresses takes place resulting in penetration of the joint. Possible explanation for the significant difference in damage area graphs between unitape and plain weave could be because of the difference in fiber strength.

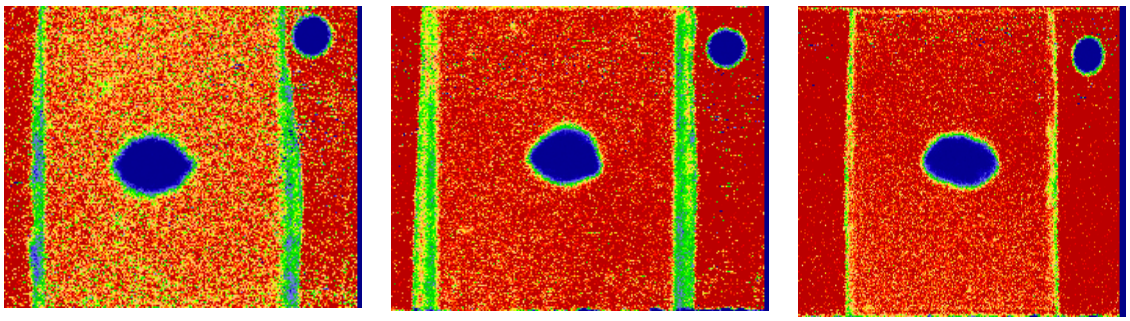

1" Impactor 40 J 0.75" Impactor 40 J 0.5" Impactor 40 J

Figure 36. Ultrasonic C-scan of glass/epoxy test coupons.

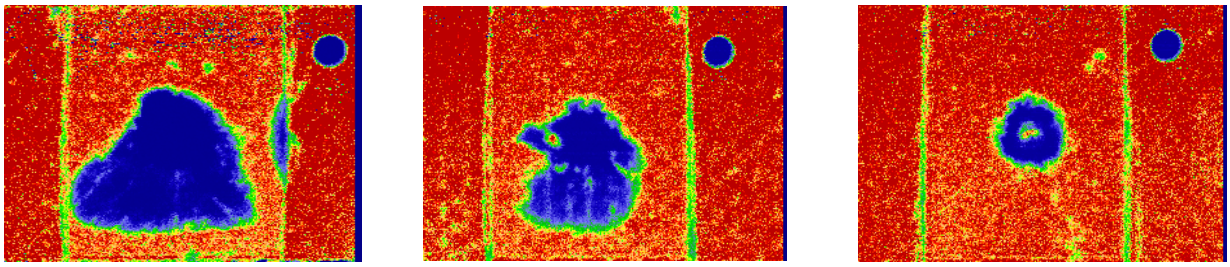

1" Impactor 40 J 0.75" Impactor 40 J 0.5" Impactor 40 J

Figure 37. Ultrasonic C-scan of carbon plain weave test coupons.

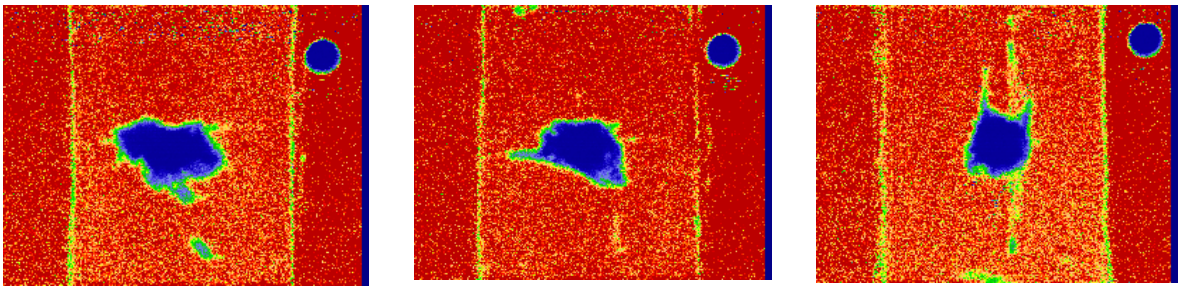

1" Impactor 40 J 0.75" Impactor 40 J 0.5" Impactor 40 J

Figure 38. Ultrasonic C-scan of carbon unitape test coupons.

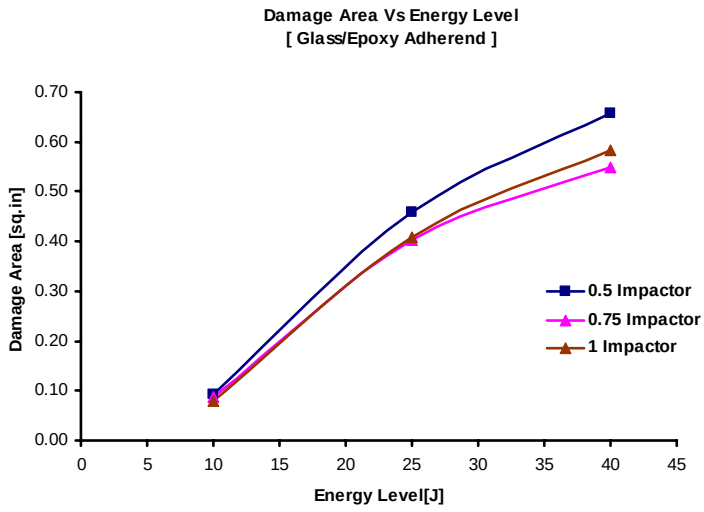

Figure 39. Plot showing relationship between damage area and energy level for woven glass/epoxy test coupons

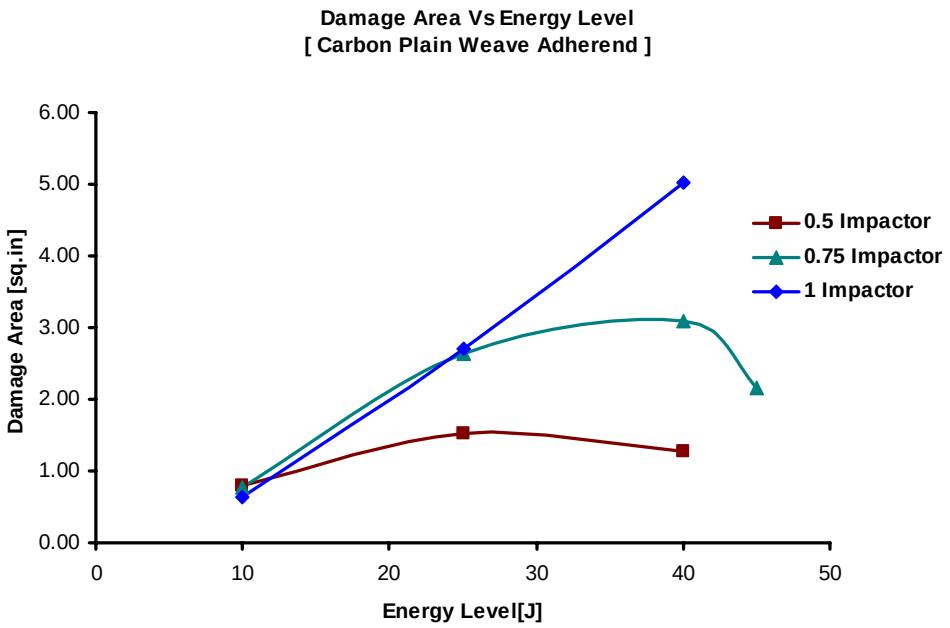

Figure 40. Plot showing relationship between damage area and energy level for carbon/epoxy plain weave fabric test coupons.

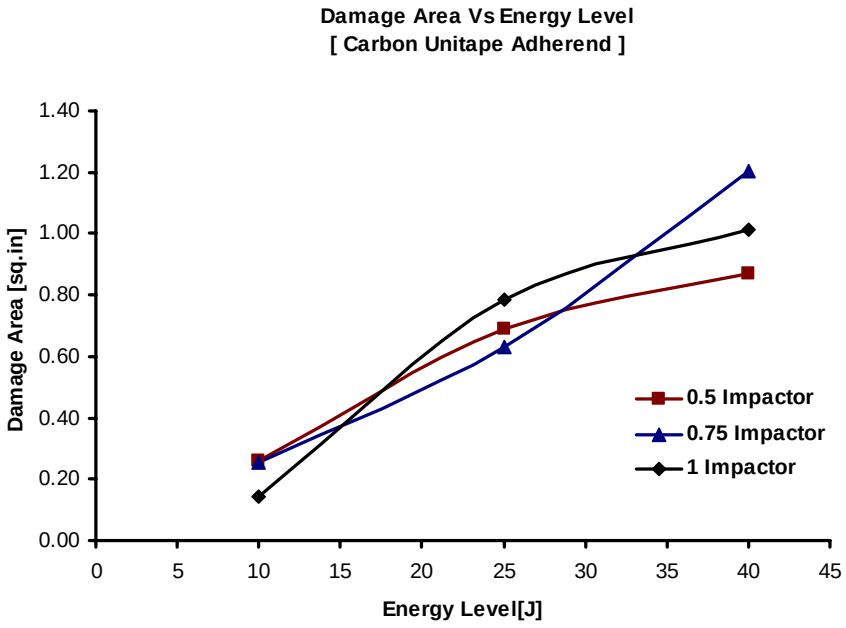

Figure 41. Plot showing relationship between damage area and energy level for carbon unitape test coupons.

Figure 42 to Figure 44 show the residual indentation induced on the test coupons on woven glass/epoxy, carbon plain weave and carbon unitape test coupons at 40J impact energy

induced by impactors of diameters 0.5″, 0.75″, 1.0″ respectively. Residual indentations are recorded by following the procedure mentioned in 6.3

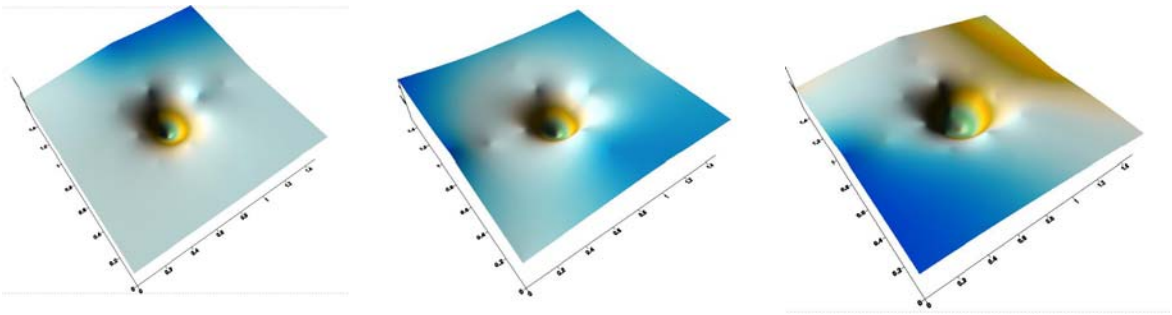

Figure 42. Surfer plots showing residual indentation on woven glass/epoxy test coupons impacted at 40J using 0.5″, 0.75″, 1.0″ impactors.

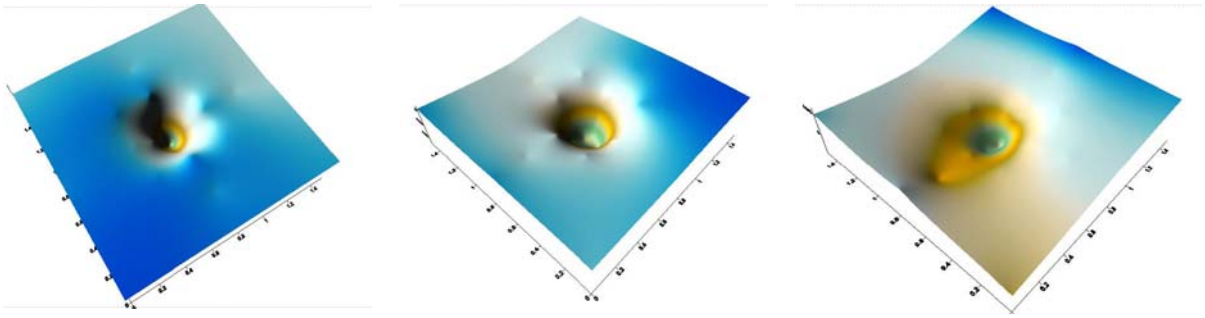

Figure 43. Surfer plots showing residual indentation on carbon/epoxy plain weave test coupons impacted at 40J using 0.5″, 0.75″, 1.0″ impactors.

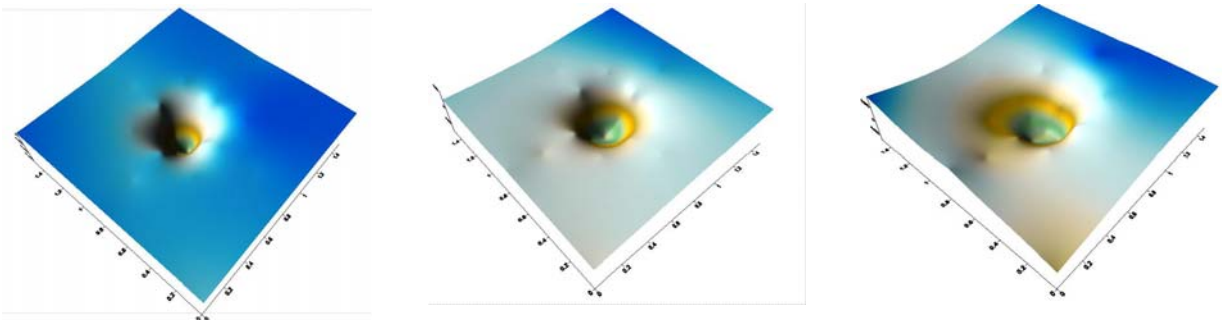

Figure 44. Surfer plots showing residual indentation on carbon unitape test coupons impacted at 40J using 0.5″, 0.75″, 1.0″ impactors.

CHAPTER 8

CONCLUSIONS AND RECOMMENDATIONS

8.1 Conclusions

Responses of adhesively bonded composite laminates to impact loading were studied experimentally. Three different adherend materials were used for the experimental study. Hysol EA 9394 was used for bonding composite laminates. Quasi-isotropic lay-up sequence was employed for the manufacture of three different adherends and all the adherends were 8 ply composite laminates. A total of 72 test coupons were impacted as well as inspected nondestructively as a part of the experimental study. All the test coupons were impacted using impactors of hemispherical cross section of having diameters 0.5″, 0.75″and 1.0″ and were impacted at 10J, 25J and 40J of impact energy.

Impact test results show that for all the three different adherend materials used for this study, larger impactor diameter produced higher impact forces as compared with impactors of smaller diameter. A significant 15% difference in the impact forces is observed between test coupons impacted with impactors of 1.0" and 0.5" diameters. It is could be observed distinctly that each material response is totally different from one another. Even though, basic trend with respect to impact force remain the same, it could be observed that drop in impact force for different impactor diameters for different materials is more for adherends made up of carbon fiber compared with adherends made up of woven glass. It could be attributed more to the material properties of the adherends. The difference in impact force between impactors gets amplified with decrease in impactor diameter and also with increase in impact energy. Another observation made in this experimental study was the impact resistance of various materials. It was observed that for a particular impactor diameter and particular impact energy, woven glass

adherends were able to withstand more impact force than adherends made up of carbon fiber. Irrespective of the adherend material, it was observed that the contact duration of impact was shorter for larger impactor diameters which were indicative of wider load distribution.

All the impacted specimens were then tested non – destructively for damage measurement. Through transmission ultrasonic C-scan method was used to quantify planar damage as well as residual indentation depth measurements were also used to quantify the damage. Both material systems showed different kind of damage states visually. In woven glass adherends, damage state observed for different impactor diameters and different energy levels visually was comparable with the damage state obtained from ultrasonic C-scanning. But in the case of carbon fiber adherends, visual the damage observed on the test coupons was not indicative of the damage state obtained through ultrasonic C-scanning. It has been observed that in glass fiber adherends, as the impactor diameter increases the damage area also increases linearly. While in carbon fiber adherends, damage area reaches a threshold value at specific impact energy level and after that propagation of damage does not take place as at higher energy levels with a specific impactor, instead formation of highly localized stresses takes place resulting in penetration of the joint. Hence forth, it can be concluded that in case of carbon fiber adherends, results obtained from visual inspection of the test coupons could be misleading and residual indentation cannot be considered as a reliable means of quantifying damage area. While comparing damage areas for woven glass/epoxy, carbon/epoxy plain weave fiber and carbon unitape test coupons, it is observed that woven glass/epoxy test coupons exhibit more impact resistance. It is also observed that the damage area observed in carbon unitape test coupons were nearly twice as that observed in woven glass/epoxy coupons. Damage area observed in

carbon/epoxy plain weave test coupons were nearly 10 times of that observed in woven glass/epoxy coupons.

From the experimental studies, it was concluded that woven glass is capable of taking more impact force than carbon fiber. Hence it is recommended that while manufacturing impact prone composite structures such as bumpers in passenger cars, it would be considered effective to manufacture impact resistant composite structures from woven glass fiber or make a hybrid structure in which woven glass fiber could be used on the outer layers of the structure and carbon fibers on the inner layers. In that way such a structure could provide impact resistance as well as strength to the structure.

8.2 Recommendations

Impact testing was done mainly at room temperature to obtain the response curves for different materials systems. It is recommended that as a part of future work, impact testing could be done on the test coupons at various environmental conditions such as hot wet, hot dry and cold wet conditions to evaluate the response of composite adhesive joints at those environmental conditions.

For this experimental study, a quasi-isotropic layup sequence was employed for the manufacture of composite joints. As a part of future work, impact testing could be done on test coupons manufactured using adherends employing different layup sequence. In addition to the above said recommendation, impact testing could also be done on adherends bonded using various types of adhesives.

LIST OF REFERENCES

REFERENCES

[1] Adams, R. D., Adhesive Bonding, CRC Press, Woodhead Publishing Limited, pp. 143-187, 2000.

[2] Adams, Robert D., and Wake, William C., Structural Adhesive Joints in Engineering, Chapman & Hall, pp.119-166, 1997.

[3] Barbero, Ever J., Introduction to Composite Materials Design, Taylor & Francis, 1998.

[4] Abrate, Serge., Impact on composite structures, Cambridge University Press, pp. 135-171, 1998.

[5] Shull, Peter J., Nondestructive Evaluation: Theory, Techniques, and Applications, Marcel Ekker Inc., pp. 17-18, 63-68, 193-194, 369-378, 597-602, 2002.

[6] Gleich, D. M., Van Tooren, M. J. L., and Buekers, A., "Structural bonded joint analysis: An overview," Adhesive Joints: Formation, Characteristics and Testing, Vol. 2, pp. 159-199.

[7] Ashcroft, I.A., Hughes, D.J., and Shaw, S.J., "Adhesive bonding of fibre reinforced polymer composite materials"

[8] Adams, R. D., "The design of adhesively bonded lap joints: Modelling Considerations," *46th International SAMPE Symposium*, May 6-10, 2001, pp. 402-414.

[9] Feraboli, Paolo J., Ireland, Donald R., and Kedward, Keith T., "The role of force and energy in low velocity impact events," *25th AIAA/ASME/ASCE/AHS/ASC Structures, Structural Dynamics & Materials Conference*, AIAA 2004-1841.

[10] Veazie, David R., and Webb, Marcus Mensah., "Low velocity impact on sandwich composites," *42nd AIAA/ASME/ASCE/AHS/ASC Structures, Structural Dynamics & Materials Conference and Exhibit*, AIAA 2001-1225.

[11] Cho, Chondgdu and Zhao, Guiping., "Effects of Geometric and Material Factors on Mechanical Response of Laminated composites due to low velocity impact," *Journal of Composite Materials*, Vol. 36, No. 12/2002.

[12] Seo, Do Won., Yoon, Ho Chei., Jeon, Yang Bae., Kim, Hyo Jin., and Lim, Jae Kyoo., "Effect of overlap length and adhesive thickness on stress distribution in adhesive bonded single-lap joints," *Key Engineering Materials* Vol. 270-273(2004) pp. 64-69.

[13] Belingardi, Giovanni., and Vadori, Roberto., "Influence of the laminate thickness in low velocity impact behaviour of composite material plate," Composite Structures 61 (2003) 27-38.

[14] Feraboli, Paolo J., and Kedward, Keith T., "Enhanced Evaluation of the low–velocity impact response of composite plates," AIAA Journal Vol.42, No. 10, Oct. 2004.

[15] Sato, Chiaki., and Iwata, Hideo., and Ikegami, Kozo., "Dynamic Deformation of Tapered Lap joint under impact loading," JSME International Journal, Series A, Vol. 40, No. 1, 1997.

[16] Farrow, I. R., Potter, K., Fisher, A., and Kelly, M., "Impact on adhesively bonded composite joints with edge effect," Advance Composite Letters, Vol. 9, No.6, 2000.

[17] Wardle, Brian L., and Lagace, Paul A., "On the behaviour of composite shells under transverse impact and quasi-static loading," AIAA-97-1059.

[18] Belingardi, Giovanni., and Vadori, Roberto., "Low velocity impact tests of laminate glass-fiber-epoxy matrix composite material plates," *International Journal of Impact Engineering* 27(2002) 213-229.

[19] Ambur, Damodar R., and Kemmerly, Heather L., "Influence of impactor mass on the damage characteristics and failure strength of laminated composite plates," AIAA 98-1784.

[20] Hosur, M.V., Alexander, J., Vaidya, U.K., and Jeelani, S., "Impact response of affordable graphite/epoxy woven fabric composites," *42nd AIAA/ASME/ASCE/AHS/ASC Structures, Structural Dynamics & Materials Conference and Exhibit*, AIAA 2001-1192.

[21] Herup, Eric J., and Palazotto, Anthony N., "Low-Velocity Impact Damage Initiation In Graphite-Epoxy/Nomex Honeycomb Sandwich Plates," AIAA-96-1519-CP.

[22] Garg, Amar C., "Prediction of Residual Strength of Impact Damaged Aerospace Composite Structures," Advanced Composites (1993).

[23] Papanicolaou, G. C., and Giannis, S. P., "The effect of low energy impact on the tensile strength of coated and uncoated glass particulate composites," *Journal of Material Science* 38 (2003) pp.533-540.

[24] Lee, Ya-Jung, and Huang, Chien-Hua., "Ultimate Strength and failure process of Composite Laminated Plates subjected to low-velocity impact," *Journal of Reinforced Plastics and Composites*, Vol. 22, No.12/2003.

[25] Yarrington, Phil, Zhang, James, and Collier, Craig and Bednarcyk, Brett A., "Failure Analysis of Adhesively Bonded Composite Joints," *46th AIAA/ASME/ASCE/AHS/ASC Structures, Structural Dynamics & Materials Conference*, AIAA 2005-2376.

[26] Benzeggagh, M. L. and Benmedakhene, S., "Residual Strength of a glass/polypropylene composite material subjected to impact," Composite Science and Technology 55 (1195) 1-11.

[27] Lal, K. M., "Residual Strength Assessment of Low velocity impact damage of graphite-epoxy laminates," Journal of Reinforced Plastics and Composites, Vol. 2- Oct 1983.

APPENDICES

APPENDIX A

IMPACT TESTING RESULTS

A. 1 IMPACT TEST RESULTS FOR WOVEN GLASS/EPOXY TEST COUPONS

TABLE 7

MAXIMUM IMPACT FORCE VALUES FOR WOVEN GLASS/EPOXY TEST COUPONS

Specimen	Thickness [in]	Impactor Diameter [in]	Target Impact Energy [in.lbf]	Measured Impact Energy [in.lbf]	Target Impact Velocity [in./min]	Measured Impact Velocity [in./min]	Maximum Force [lbf]
I1G31C1	0.1890	1.00	354.00	350.08	8435.07	8385.48	2206.96
I1G21C2	0.1900	1.00	354.00	355.08	8368.82	8378.71	2172.59
I1G61C3	0.1875	1.00	354.00	354.87	8368.82	8376.30	2253.220
I1G31B1	0.1890	1.00	221.00	220.96	6612.39	6609.54	1866.670
I1G71B2	0.1900	1.00	221.00	222.18	6612.39	6627.74	1399.570
I1G31B3	0.1890	1.00	221.00	222.16	6612.39	6627.53	1803.160
I1G61A1	0.1875	1.00	88.50	91.49	4184.41	4253.18	1308.110
I1G61A2	0.1875	1.00	88.50	89.72	4184.41	4211.85	1302.250
I1G22C1	0.1900	0.75	354.00	353.01	8416.85	8402.30	2124.670
I1G62C2	0.1875	0.75	354.00	352.49	8416.85	8396.05	2188.580
I1G22C3	0.1900	0.75	354.00	352.79	8416.85	8399.60	2118.340
I1G32B1	0.1890	0.75	221.00	224.69	6650.34	6703.43	1853.010
I1G42B2	0.1885	0.75	221.00	221.67	6650.34	6658.15	1888.050
I1G42B3	0.1885	0.75	221.00	221.11	6650.34	6649.78	1871.840
I1G42A1	0.1885	0.75	88.50	82.08	4208.42	4051.62	1191.180
I1G42A2	0.1885	0.75	88.50	91.63	4208.42	4280.69	1261.370
I1G53C2	0.1933	0.50	354.00	355.40	8435.07	8448.95	1951.390
I1G83C3	0.1900	0.50	354.00	357.78	8435.07	8483.58	1904.920
I1G53C4	0.1933	0.50	354.00	358.20	8441.17	8488.51	1904.230
I1G53B1	0.1933	0.50	221.00	222.18	6664.74	6680.21	1789.410
I1G53B4	0.1933	0.50	221.00	224.95	6669.56	6726.94	1783.070
I1G73B5	0.1900	0.50	221.00	224.51	6669.56	6720.34	1787.250
I1G73A3	0.1900	0.50	88.50	87.44	4220.59	4194.06	1201.710
I1G73A2	0.1900	0.50	88.50	91.33	4220.59	4286.31	1114.890

TABLE 8

TOTAL ENERGY VALUES FOR WOVEN GLASS/ EPOXY TEST COUPONS

Specimen	Thickness [in]	Impactor Diameter [in]	Target Impact Energy [in.lbf]	Measured Impact Energy [in.lbf]	Target Impact Velocity [in./min]	Measured Impact Velocity [in./min]	Total Energy [in-lbf]
I1G31C1	0.1890	1.00	354.00	350.08	8435.07	8385.48	194.67
I1G21C2	0.1900	1.00	354.00	355.08	8368.82	8378.71	196.89
I1G61C3	0.1875	1.00	354.00	354.87	8368.82	8376.30	199.240
I1G31B1	0.1890	1.00	221.00	220.96	6612.39	6609.54	104.500
I1G71B2	0.1900	1.00	221.00	222.18	6612.39	6627.74	134.600
I1G31B3	0.1890	1.00	221.00	222.16	6612.39	6627.53	110.840
I1G61A1	0.1875	1.00	88.50	91.49	4184.41	4253.18	31.280
I1G61A2	0.1875	1.00	88.50	89.72	4184.41	4211.85	30.300
I1G22C1	0.1900	0.75	354.00	353.01	8416.85	8402.30	192.560
I1G62C2	0.1875	0.75	354.00	352.49	8416.85	8396.05	193.920
I1G22C3	0.1900	0.75	354.00	352.79	8416.85	8399.60	195.490
I1G32B1	0.1890	0.75	221.00	224.69	6650.34	6703.43	105.620
I1G42B2	0.1885	0.75	221.00	221.67	6650.34	6658.15	93.170
I1G42B3	0.1885	0.75	221.00	221.11	6650.34	6649.78	92.820
I1G42A1	0.1885	0.75	88.50	82.08	4208.42	4051.62	26.580
I1G42A2	0.1885	0.75	88.50	91.63	4208.42	4280.69	27.600
I1G53C2	0.1933	0.50	354.00	355.40	8435.07	8448.95	249.320
I1G83C3	0.1900	0.50	354.00	357.78	8435.07	8483.58	209.280
I1G53C4	0.1933	0.50	354.00	358.20	8441.17	8488.51	217.770
I1G53B1	0.1933	0.50	221.00	222.18	6664.74	6680.21	107.830
I1G53B4	0.1900	0.50	221.00	224.95	6669.56	6726.94	107.830
I1G73B5	0.1900	0.50	221.00	224.51	6669.56	6720.34	110.400
I1G73A3	0.1900	0.50	88.50	87.44	4220.59	4194.06	26.770
I1G73A2	0.1900	0.50	88.50	91.33	4220.59	4286.31	27.810

TABLE 9

DAMAGE AREA VALUES FOR WOVEN GLASS/EPOXY TEST COUPONS

Specimen	Thickness [in]	Impactor Diameter [in]	Target Impact Energy [in.lbf]	Measured Impact Energy [in.lbf]	Target Impact Velocity [in./min]	Measured Impact Velocity [in./min]	Damage Area [in^2]
I1G31C1	0.1890	1.00	354.00	350.08	8435.07	8385.48	0.6064
I1G21C2	0.1900	1.00	354.00	355.08	8368.82	8378.71	0.5500
I1G61C3	0.1875	1.00	354.00	354.87	8368.82	8376.30	0.5496
I1G31B1	0.1890	1.00	221.00	220.96	6612.39	6609.54	0.4584
I1G71B2	0.1900	1.00	221.00	222.18	6612.39	6627.74	0.4260
I1G31B3	0.1890	1.00	221.00	222.16	6612.39	6627.53	0.3780
I1G61A1	0.1875	1.00	88.50	91.49	4184.41	4253.18	0.0784
I1G61A2	0.1875	1.00	88.50	89.72	4184.41	4211.85	0.0976
I1G22C1	0.1900	0.75	354.00	353.01	8416.85	8402.30	0.5224
I1G62C2	0.1875	0.75	354.00	352.49	8416.85	8396.05	0.5528
I1G22C3	0.1900	0.75	354.00	352.79	8416.85	8399.60	0.5496
I1G32B1	0.1890	0.75	221.00	224.69	6650.34	6703.43	0.4240
I1G42B2	0.1885	0.75	221.00	221.67	6650.34	6658.15	0.4188
I1G42B3	0.1885	0.75	221.00	221.11	6650.34	6649.78	0.3816
I1G42A1	0.1885	0.75	88.50	82.08	4208.42	4051.62	0.0921
I1G42A2	0.1885	0.75	88.50	91.63	4208.42	4280.69	0.0871
I1G53C2	0.1933	0.50	354.00	355.40	8435.07	8448.95	0.6542
I1G83C3	0.1900	0.50	354.00	357.78	8435.07	8483.58	0.6412
I1G53C4	0.1933	0.50	354.00	358.20	8441.17	8488.51	0.6768
I1G53B1	0.1933	0.50	221.00	222.18	6664.74	6680.21	0.5160
I1G53B4	0.1900	0.50	221.00	224.95	6669.56	6726.94	0.4696
I1G73B5	0.1900	0.50	221.00	224.51	6669.56	6720.34	0.3884
I1G73A3	0.1900	0.50	88.50	87.44	4220.59	4194.06	0.0952
I1G73A2	0.1900	0.50	88.50	91.33	4220.59	4286.31	0.0919

TABLE 10

RESIDUAL INDENTATION DEPTH VALUES FOR WOVEN GLASS/EPOXY TEST COUPONS

Specimen	Thickness [in]	Impactor Diameter [in]	Target Impact Energy [in.lbf]	Measured Impact Energy [in.lbf]	Target Impact Velocity [in./min]	Measured Impact Velocity [in./min]	Max Surface Indentation [in]
I1G31C1	0.1890	1.00	354.00	350.08	8435.07	8385.48	0.0095
I1G21C2	0.1900	1.00	354.00	355.08	8368.82	8378.71	0.0125
I1G61C3	0.1875	1.00	354.00	354.87	8368.82	8376.30	0.0090
I1G31B1	0.1890	1.00	221.00	220.96	6612.39	6609.54	0.0065
I1G71B2	0.1900	1.00	221.00	222.18	6612.39	6627.74	0.0110
I1G31B3	0.1890	1.00	221.00	222.16	6612.39	6627.53	0.0030
I1G61A1	0.1875	1.00	88.50	91.49	4184.41	4253.18	_____
I1G61A2	0.1875	1.00	88.50	89.72	4184.41	4211.85	_____
I1G22C1	0.1900	0.75	354.00	353.01	8416.85	8402.30	0.0100
I1G62C2	0.1875	0.75	354.00	352.49	8416.85	8396.05	0.0025
I1G22C3	0.1900	0.75	354.00	352.79	8416.85	8399.60	0.0070
I1G32B1	0.1890	0.75	221.00	224.69	6650.34	6703.43	0.0035
I1G42B2	0.1885	0.75	221.00	221.67	6650.34	6658.15	0.0015
I1G42B3	0.1885	0.75	221.00	221.11	6650.34	6649.78	0.0070
I1G42A1	0.1885	0.75	88.50	82.08	4208.42	4051.62	_____
I1G42A2	0.1885	0.75	88.50	91.63	4208.42	4280.69	_____
I1G53C2	0.1933	0.50	354.00	355.40	8435.07	8448.95	0.0080
I1G83C3	0.1900	0.50	354.00	357.78	8435.07	8483.58	0.0135
I1G53C4	0.1933	0.50	354.00	358.20	8441.17	8488.51	0.0095
I1G53B1	0.1933	0.50	221.00	222.18	6664.74	6680.21	0.0010
I1G53B4	0.1900	0.50	221.00	224.95	6669.56	6726.94	0.0130
I1G73B5	0.1900	0.50	221.00	224.51	6669.56	6720.34	0.0005
I1G73A3	0.1900	0.50	88.50	87.44	4220.59	4194.06	_____
I1G73A2	0.1900	0.50	88.50	91.33	4220.59	4286.31	_____

A. 2 IMPACT TEST RESULTS FOR CARBON/EPOXY PLAIN WEAVE TEST COUPONS

TABLE 11

MAXIMUM IMPACT FORCE VALUES FOR CARBON/EPOXY PLAIN WEAVE TEST COUPONS

Specimen	Thickness [in]	Impactor Diameter [in]	Target Impact Energy [in.lbf]	Measured Impact Energy [in.lbf]	Target Impact Velocity [in./min]	Measured Impact Velocity [in./min]	Maximum Force [lbf]
I1P41C1	0.1505	1.00	354.00	356.25	8362.87	8386.61	2243.930
I1P91C2	0.1423	1.00	354.00	351.56	8368.82	8337.19	2423.090
I1P11C3	0.1422	1.00	354.00	353.83	8368.82	8363.96	2203.900
I1P61B1	0.1467	1.00	221.00	220.45	6612.39	6601.98	1886.080
I1P61B2	0.1467	1.00	221.00	220.26	6612.39	6599.09	1911.070
I1P61B3	0.1467	1.00	221.00	219.86	6612.39	6593.06	1962.450
I1P41A1	0.1505	1.00	88.50	89.43	4184.41	4204.86	1207.830
I1P81A2	0.1477	1.00	88.50	88.83	4184.41	4190.80	1190.350
I1P52C1	0.1482	0.75	354.00	351.76	8419.88	8390.72	2035.590
I1P62C2	0.1467	0.75	354.00	355.33	8419.88	8433.20	1987.060
I1P52C3	0.1482	0.75	354.00	353.72	8419.88	8414.01	1937.040
I1P92B1	0.1423	0.75	221.00	220.71	6652.73	6646.36	1877.270
I1P52B2	0.1483	0.75	221.00	220.17	6652.73	6638.18	1850.280
I1P52B3	0.1483	0.75	221.00	220.42	6652.73	6642.07	1901.830
I1P92A1	0.1423	0.75	88.50	88.88	4209.94	4217.68	1164.930
I1P92A2	0.1423	0.75	88.50	88.92	4209.94	4218.71	1148.910
I1P43C1	0.1505	0.50	354.00	353.99	8441.17	8438.52	1689.140
I1P43C2	0.1505	0.50	354.00	353.83	8435.07	8430.27	1572.840
I1P83C3	0.1477	0.50	354.00	354.63	8441.17	8446.19	1727.530
I1P23B1	0.1495	0.50	221.00	220.56	6669.56	6660.91	1709.660
I1P23B2	0.1495	0.50	221.00	220.30	6669.56	6657.00	1627.500
I1P43B4	0.1464	0.50	221.00	224.52	6664.74	6715.31	1596.910
I1P23A1	0.1500	0.50	88.50	89.38	4220.59	4240.25	1145.000
I1P13A2	0.1422	0.50	88.50	88.82	4220.59	4227.03	1138.630

TABLE 12

TOTAL ENERGY VALUES FOR CARBON/EPOXY PLAIN WEAVE TEST COUPONS

Specimen	Thickness [in]	Impactor Diameter [in]	Target Impact Energy [in.lbf]	Measured Impact Energy [in.lbf]	Target Impact Velocity [in./min]	Measured Impact Velocity [in./min]	Total Energy [in-lbf]
I1P41C1	0.1505	1.00	354.00	356.25	8362.87	8386.61	217.130
I1P91C2	0.1423	1.00	354.00	351.56	8368.82	8337.19	183.240
I1P11C3	0.1422	1.00	354.00	353.83	8368.82	8363.96	203.180
I1P61B1	0.1467	1.00	221.00	220.45	6612.39	6601.98	113.020
I1P61B2	0.1467	1.00	221.00	220.26	6612.39	6599.09	105.640
I1P61B3	0.1467	1.00	221.00	219.86	6612.39	6593.06	106.540
I1P41A1	0.1505	1.00	88.50	89.43	4184.41	4204.86	42.370
I1P81A2	0.1477	1.00	88.50	88.83	4184.41	4190.80	40.420
I1P52C1	0.1482	0.75	354.00	351.76	8419.88	8390.72	262.110
I1P62C2	0.1467	0.75	354.00	355.33	8419.88	8433.20	253.680
I1P52C3	0.1482	0.75	354.00	353.72	8419.88	8414.01	284.870
I1P92B1	0.1423	0.75	221.00	220.71	6652.73	6646.36	109.010
I1P52B2	0.1483	0.75	221.00	220.17	6652.73	6638.18	107.140
I1P52B3	0.1483	0.75	221.00	220.42	6652.73	6642.07	107.800
I1P92A1	0.1423	0.75	88.50	88.88	4209.94	4217.68	38.510
I1P92A2	0.1423	0.75	88.50	88.92	4209.94	4218.71	39.930
I1P43C1	0.1505	0.50	354.00	353.99	8441.17	8438.52	317.060
I1P43C2	0.1505	0.50	354.00	353.83	8435.07	8430.27	333.630
I1P83C3	0.1477	0.50	354.00	354.63	8441.17	8446.19	350.820
I1P23B1	0.1495	0.50	221.00	220.56	6669.56	6660.91	146.310
I1P23B2	0.1495	0.50	221.00	220.30	6669.56	6657.00	143.030
I1P43B4	0.1464	0.50	221.00	224.52	6664.74	6715.31	128.190
I1P23A1	0.1500	0.50	88.50	89.38	4220.59	4240.25	38.660
I1P13A2	0.1422	0.50	88.50	88.82	4220.59	4227.03	37.830

TABLE 13

DAMAGE AREA VALUES FOR CARBON/EPOXY PLAIN WEAVE TEST COUPONS

Specimen	Thickness [in]	Impactor Diameter [in]	Target Impact Energy [in.lbf]	Measured Impact Energy [in.lbf]	Target Impact Velocity [in./min]	Measured Impact Velocity [in./min]	Damage Area [in^2]
I1P41C1	0.1505	1.00	354.00	356.25	8362.87	8386.61	4.2128
I1P91C2	0.1423	1.00	354.00	351.56	8368.82	8337.19	5.7816
I1P11C3	0.1422	1.00	354.00	353.83	8368.82	8363.96	5.0980
I1P61B1	0.1467	1.00	221.00	220.45	6612.39	6601.98	1.6848
I1P61B2	0.1467	1.00	221.00	220.26	6612.39	6599.09	3.3776
I1P61B3	0.1467	1.00	221.00	219.86	6612.39	6593.06	3.0636
I1P41A1	0.1505	1.00	88.50	89.43	4184.41	4204.86	0.6452
I1P81A2	0.1477	1.00	88.50	88.83	4184.41	4190.80	0.6404
I1P52C1	0.1482	0.75	354.00	351.76	8419.88	8390.72	3.0024
I1P62C2	0.1467	0.75	354.00	355.33	8419.88	8433.20	3.7424
I1P52C3	0.1482	0.75	354.00	353.72	8419.88	8414.01	2.5616
I1P92B1	0.1423	0.75	221.00	220.71	6652.73	6646.36	3.4088
I1P52B2	0.1483	0.75	221.00	220.17	6652.73	6638.18	2.9804
I1P52B3	0.1483	0.75	221.00	220.42	6652.73	6642.07	1.5264
I1P92A1	0.1423	0.75	88.50	88.88	4209.94	4217.68	0.6696
I1P92A2	0.1423	0.75	88.50	88.92	4209.94	4218.71	0.8640
I1P43C1	0.1505	0.50	354.00	353.99	8441.17	8438.52	1.3772
I1P43C2	0.1505	0.50	354.00	353.83	8435.07	8430.27	0.8892
I1P83C3	0.1477	0.50	354.00	354.63	8441.17	8446.19	1.5452
I1P23B1	0.1495	0.50	221.00	220.56	6669.56	6660.91	1.8876
I1P23B2	0.1495	0.50	221.00	220.30	6669.56	6657.00	1.5124
I1P43B4	0.1464	0.50	221.00	224.52	6664.74	6715.31	1.1600
I1P23A1	0.1500	0.50	88.50	89.38	4220.59	4240.25	0.7984
I1P13A2	0.1422	0.50	88.50	88.82	4220.59	4227.03	0.8084

TABLE 14

RESIDUAL INDENTATION DEPTH VALUES FOR CARBON/EPOXY PLAIN WEAVE TEST COUPONS

Specimen	Thickness [in]	Impactor Diameter [in]	Target Impact Energy [in.lbf]	Measured Impact Energy [in.lbf]	Target Impact Velocity [in./min]	Measured Impact Velocity [in./min]	Max Surface Indentation [in]
I1P41C1	0.1505	1.00	354.00	356.25	8362.87	8386.61	0.005
I1P91C2	0.1423	1.00	354.00	351.56	8368.82	8337.19	0.005
I1P11C3	0.1422	1.00	354.00	353.83	8368.82	8363.96	0.0080
I1P61B1	0.1467	1.00	221.00	219.86	6612.39	6593.06	0.0015
I1P61B2	0.1467	1.00	221.00	220.26	6612.39	6599.09	0.0010
I1P61B3	0.1467	1.00	221.00	219.86	6612.39	6593.06	0.0095
I1P41A1	0.1505	1.00	88.50	89.43	4184.41	4204.86	_____
I1P81A2	0.1477	1.00	88.50	88.83	4184.41	4190.80	_____
I1P52C1	0.1482	0.75	354.00	351.76	8419.88	8390.72	0.0240
I1P62C2	0.1467	0.75	354.00	355.33	8419.88	8433.20	0.0140
I1P52C3	0.1482	0.75	354.00	353.72	8419.88	8414.01	0.0265
I1P92B1	0.1423	0.75	221.00	220.71	6652.73	6646.36	0.0010
I1P52B2	0.1483	0.75	221.00	220.17	6652.73	6638.18	0.0110
I1P52B3	0.1483	0.75	221.00	220.42	6652.73	6642.07	0.0005
I1P92A1	0.1423	0.75	88.50	88.88	4209.94	4217.68	_____
I1P92A2	0.1423	0.75	88.50	88.92	4209.94	4218.71	_____
I1P43C1	0.1505	0.50	354.00	353.99	8441.17	8438.52	0.0730
I1P43C2	0.1505	0.50	354.00	353.83	8435.07	8430.27	0.0900
I1P83C3	0.1477	0.50	354.00	354.63	8441.17	8446.19	0.1325
I1P23B1	0.1495	0.50	221.00	220.56	6669.56	6660.91	0.0100
I1P23B2	0.1495	0.50	221.00	220.30	6669.56	6657.00	0.0130
I1P43B4	0.1464	0.50	221.00	224.52	6664.74	6715.31	0.0035
I1P23A1	0.1500	0.50	88.50	89.38	4220.59	4240.25	_____
I1P13A2	0.1422	0.50	88.50	88.82	4220.59	4227.03	_____

A.3 IMPACT TEST RESULTS FOR CARBON UNITAPE TEST COUPONS

TABLE 15

MAXIMUM IMPACT FORCE VALUES FOR CARBON UNITAPE TEST COUPONS

Specimen	Thickness [in]	Impactor Diameter [in]	Target Impact Energy [in.lbf]	Measured Impact Energy [in.lbf]	Target Impact Velocity [in./min]	Measured Impact Velocity [in./min]	Maximum Force [lbf]
I1U31C1	0.1310	1.00	354.0	352.17	8368.82	8344.35	2053.210
I1U31C2	0.1310	1.00	354.0	353.90	8368.82	8364.86	2225.470
I1U51C4	0.1337	1.00	354.0	356.93	8362.87	8394.65	2286.950
I1U21B1	0.1302	1.00	221.0	218.79	6612.39	6577.07	1921.660
I1U21B2	0.1302	1.00	221.0	220.340	6612.39	6600.30	1922.700
I1U21B3	0.1350	1.00	221.0	217.460	6612.39	6556.99	2059.540
I1U61A1	0.1350	1.00	88.5	90.660	4184.41	4233.73	1259.690
I1U21A2	0.1291	1.00	88.5	88.40	4184.41	4180.55	1276.100
I1U72C1	0.1317	0.75	354.0	350.91	8419.88	8380.50	1899.430
I1U42C2	0.1328	0.75	354.0	354.06	8419.88	8418.12	1966.760
I1U42C3	0.1328	0.75	354.0	353.80	8419.88	8415.01	1952.030
I1U12B1	0.1326	0.75	221.0	220.68	6652.73	6645.88	1804.190
I1U12B2	0.1326	0.75	221.0	219.98	6652.73	6635.44	1855.690
I1U12B3	0.1326	0.75	221.0	219.62	6652.73	6629.88	1775.380
I1U12A1	0.1292	0.75	88.5	89.33	4209.94	4228.40	1254.600
I1U52A2	0.1337	0.75	88.5	89.42	4209.94	4230.50	1236.170
I1U53C1	0.1339	0.50	354.0	355.86	8435.07	8454.32	1590.870
I1U73C2	0.1324	0.50	354.0	353.59	8441.17	8433.79	1593.400
I1U53C3	0.1339	0.50	354.0	352.68	8441.17	8422.92	1661.710
I1U43B1	0.1325	0.50	221.0	222.08	6669.56	6683.79	1530.150
I1U73B2	0.1317	0.50	221.0	222.39	6669.56	6688.53	1591.690
I1U33B3	0.1335	0.50	221.0	222.32	6664.74	6682.35	1541.890
I1U63A1	0.1351	0.50	88.5	89.33	4220.59	4239.02	1153.240
I1U63A2	0.1351	0.50	88.5	89.49	4220.59	4242.88	1217.020

TABLE 16

TOTAL ENERGY VALUES FOR CARBON UNITAPE TEST COUPONS

Specimen	Thickness [in]	Impactor Diameter [in]	Target Impact Energy [in.lbf]	Measured Impact Energy [in.lbf]	Target Impact Velocity [in./min]	Measured Impact Velocity [in./min]	Total Energy [in-lbf]
I1U31C1	0.1310	1.00	354.0	352.17	8368.81786	8344.35	220.890
I1U31C2	0.1310	1.00	354.0	353.90	8368.82	8364.86	221.430
I1U51C4	0.1337	1.00	354.0	356.93	8362.87	8394.65	188.520
I1U21B1	0.1302	1.00	221.0	218.79	6612.39	6577.07	121.180
I1U21B2	0.1302	1.00	221.0	220.340	6612.39	6600.30	128.520
I1U21B3	0.1350	1.00	221.0	217.460	6612.39	6556.99	123.970
I1U61A1	0.1350	1.00	88.5	90.660	4184.41	4233.73	36.920
I1U21A2	0.1291	1.00	88.5	88.40	4184.41	4180.55	34.040
I1U72C1	0.1317	0.75	354.0	350.91	8419.88	8380.50	252.000
I1U42C2	0.1328	0.75	354.0	354.06	8419.88	8418.12	235.440
I1U42C3	0.1328	0.75	354.0	353.80	8419.88	8415.01	272.560
I1U12B1	0.1326	0.75	221.0	220.68	6652.73	6645.88	123.230
I1U12B2	0.1326	0.75	221.0	219.98	6652.73	6635.44	126.210
I1U12B3	0.1326	0.75	221.0	219.62	6652.73	6629.88	121.020
I1U12A1	0.1292	0.75	88.5	89.33	4209.94	4228.40	38.020
I1U52A2	0.1337	0.75	88.5	89.42	4209.94	4230.50	34.790
I1U53C1	0.1339	0.50	354.0	355.86	8435.07	8454.32	314.690
I1U73C2	0.1324	0.50	354.0	353.59	8441.17	8433.79	295.000
I1U53C3	0.1339	0.50	354.0	352.68	8441.17	8422.92	324.070
I1U43B1	0.1325	0.50	221.0	222.08	6669.56	6683.79	121.990
I1U73B2	0.1317	0.50	221.0	222.39	6669.56	6688.53	142.030
I1U33B3	0.1335	0.50	221.0	222.32	6664.74	6682.35	132.920
I1U63A1	0.1351	0.50	88.5	89.33	4220.59	4239.02	35.070
I1U63A2	0.1351	0.50	88.5	89.49	4220.59	4242.88	35.340

TABLE 17

DAMAGE AREA VALUES FOR CARBON UNITAPE TEST COUPONS

Specimen	Thickness [in]	Impactor Diameter [in]	Target Impact Energy [in.lbf]	Measured Impact Energy [in.lbf]	Target Impact Velocity [in./min]	Measured Impact Velocity [in./min]	Damage Area [in^2]
I1U31C1	0.1310	1.00	354.0	352.17	8368.81786	8344.35	0.9072
I1U31C2	0.1310	1.00	354.0	353.90	8368.82	8364.86	1.1660
I1U51C4	0.1337	1.00	354.0	356.93	8362.87	8394.65	0.9716
I1U21B1	0.1302	1.00	221.0	218.79	6612.39	6577.07	0.5996
I1U21B2	0.1302	1.00	221.0	220.340	6612.39	6600.30	0.7528
I1U21B3	0.1350	1.00	221.0	217.460	6612.39	6556.99	1.0004
I1U61A1	0.1350	1.00	88.5	90.660	4184.41	4233.73	0.1200
I1U21A2	0.1291	1.00	88.5	88.40	4184.41	4180.55	0.0976
I1U72C1	0.1317	0.75	354.0	350.91	8419.88	8380.50	1.0280
I1U42C2	0.1328	0.75	354.0	354.06	8419.88	8418.12	1.3552
I1U42C3	0.1328	0.75	354.0	353.80	8419.88	8415.01	1.2244
I1U12B1	0.1326	0.75	221.0	220.68	6652.73	6645.88	0.6372
I1U12B2	0.1326	0.75	221.0	219.98	6652.73	6635.44	0.6008
I1U12B3	0.1326	0.75	221.0	219.62	6652.73	6629.88	0.6228
I1U12A1	0.1292	0.75	88.5	89.33	4209.94	4228.40	0.2556
I1U52A2	0.1337	0.75	88.5	89.42	4209.94	4230.50	0.3186
I1U53C1	0.1339	0.50	354.0	355.86	8435.07	8454.32	0.7528
I1U73C2	0.1324	0.50	354.0	353.59	8441.17	8433.79	0.8640
I1U53C3	0.1339	0.50	354.0	352.68	8441.17	8422.92	0.9940
I1U43B1	0.1325	0.50	221.0	222.08	6669.56	6683.79	0.8060
I1U73B2	0.1317	0.50	221.0	222.39	6669.56	6688.53	0.6780
I1U33B3	0.1335	0.50	221.0	222.32	6664.74	6682.35	0.5824
I1U63A1	0.1351	0.50	88.5	89.33	4220.59	4239.02	0.3568
I1U63A2	0.1351	0.50	88.5	89.49	4220.59	4242.88	0.2612

TABLE 18

RESIDUAL INDENTATION DEPTH VALUES FOR CARBON UNITAPE TEST COUPONS

Specimen	Thickness [in]	Impactor Diameter [in]	Target Impact Energy [in.lbf]	Measured Impact Energy [in.lbf]	Target Impact Velocity [in./min]	Measured Impact Velocity [in./min]	Max Surface Indentation [in]
I1U31C1	0.1310	1.00	354.0	352.17	8368.818	8344.35	0.005
I1U31C2	0.1310	1.00	354.0	353.90	8368.82	8364.86	0.0065
I1U51C4	0.1337	1.00	354.0	356.93	8362.87	8394.65	0.0100
I1U21B1	0.1302	1.00	221.0	218.79	6612.39	6577.07	0.0020
I1U21B2	0.1302	1.00	221.0	220.340	6612.39	6600.30	0.0075
I1U21B3	0.1350	1.00	221.0	217.460	6612.39	6556.99	0.0105
I1U61A1	0.1350	1.00	88.5	90.660	4184.41	4233.73	_____
I1U21A2	0.1291	1.00	88.5	88.40	4184.41	4180.55	_____
I1U72C1	0.1317	0.75	354.0	350.91	8419.88	8380.50	0.0150
I1U42C2	0.1328	0.75	354.0	354.06	8419.88	8418.12	0.0155
I1U42C3	0.1328	0.75	354.0	353.80	8419.88	8415.01	0.0205
I1U12B1	0.1326	0.75	221.0	220.68	6652.73	6645.88	0.0035
I1U12B2	0.1326	0.75	221.0	219.98	6652.73	6635.44	0.0095
I1U12B3	0.1326	0.75	221.0	219.62	6652.73	6629.88	0.0065
I1U12A1	0.1292	0.75	88.5	89.33	4209.94	4228.40	_____
I1U52A2	0.1337	0.75	88.5	89.42	4209.94	4230.50	_____
I1U53C1	0.1339	0.50	354.0	355.86	8435.07	8454.32	0.0635
I1U73C2	0.1324	0.50	354.0	353.59	8441.17	8433.79	0.0665
I1U53C3	0.1339	0.50	354.0	352.68	8441.17	8422.92	0.1315
I1U43B1	0.1325	0.50	221.0	222.08	6669.56	6683.79	0.0065
I1U73B2	0.1317	0.50	221.0	222.39	6669.56	6688.53	0.0140
I1U33B3	0.1335	0.50	221.0	222.32	6664.74	6682.35	0.0125
I1U63A1	0.1351	0.50	88.5	89.33	4220.59	4239.02	_____
I1U63A2	0.1351	0.50	88.5	89.49	4220.59	4242.88	_____

A. 4 FORCE DISPLACEMENT PLOTS OF TEST COUPONS IMPACTED AT 25 J

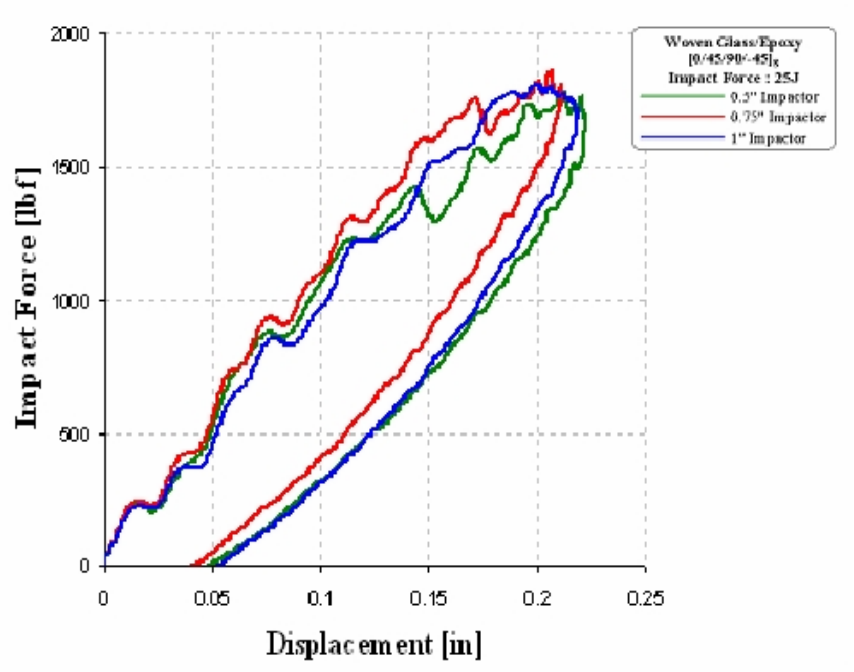

Figure 45. Typical Force Displacement plot of a woven glass/epoxy test coupon impacted at 25J.

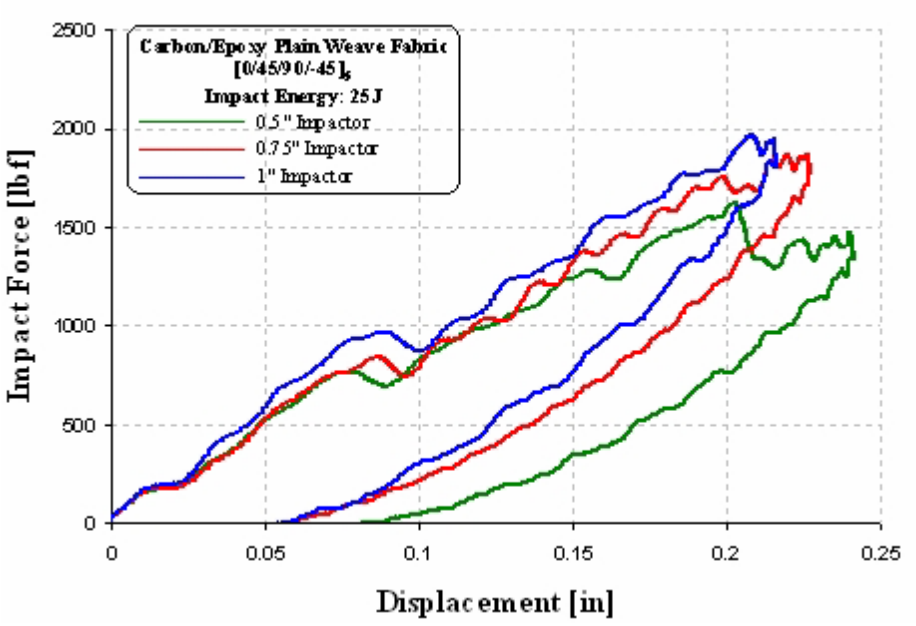

Figure 46. Typical Force Displacement plot of a carbon/epoxy plain weave test coupon impacted at 25J.

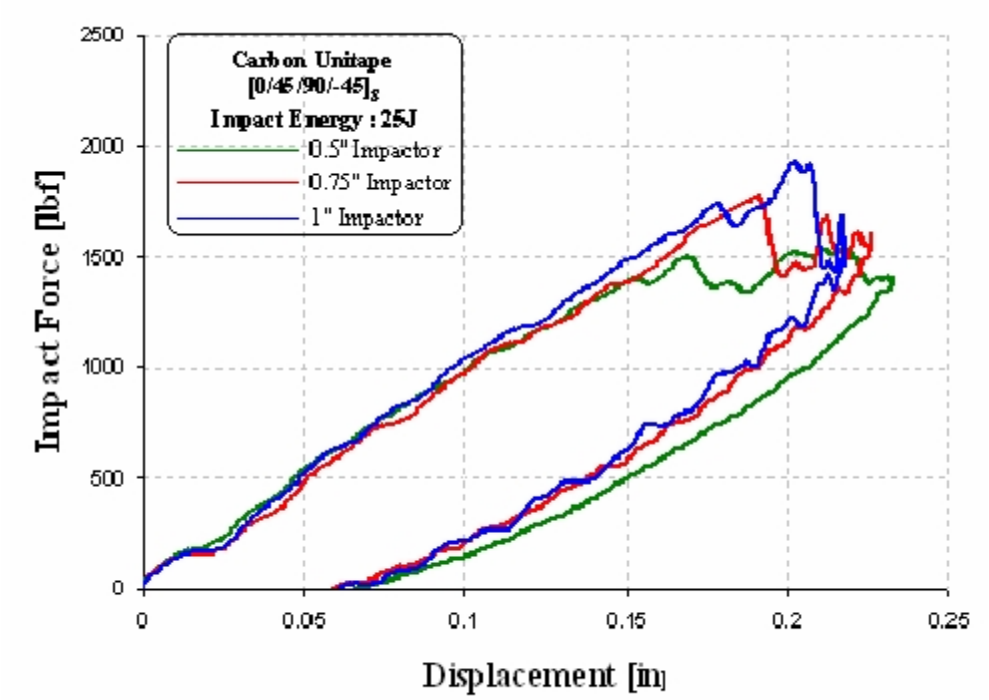

Figure 47. Typical Force Displacement plot of a carbon unitape test coupon impacted at 25J.

A. 5 FORCE DISPLACEMENT PLOTS OF TEST COUPONS IMPACTED AT 10 J

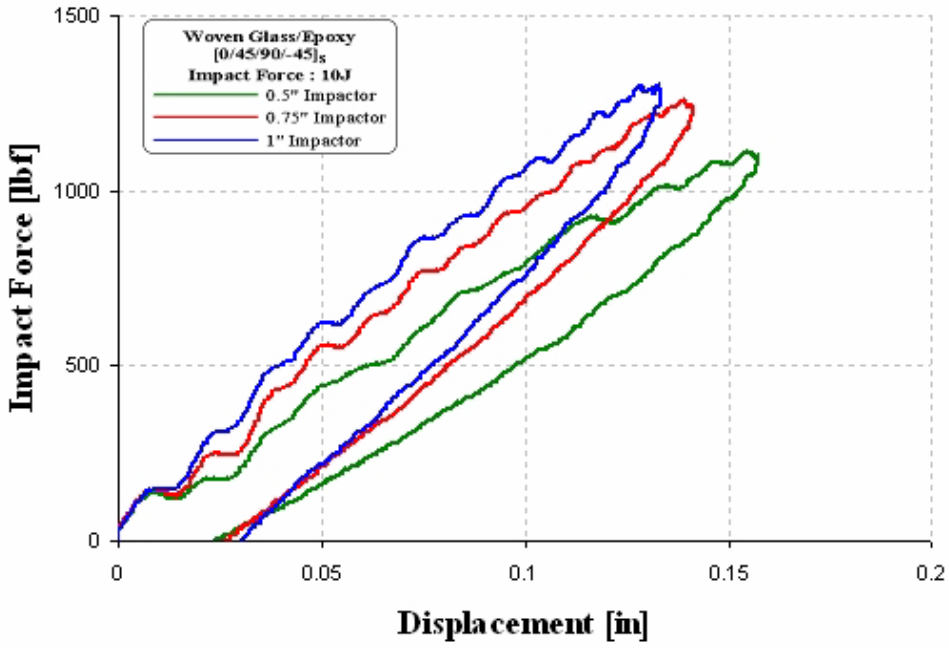

Figure 48. Typical Force Displacement plot of a woven glass/epoxy test coupon impacted at 10J.

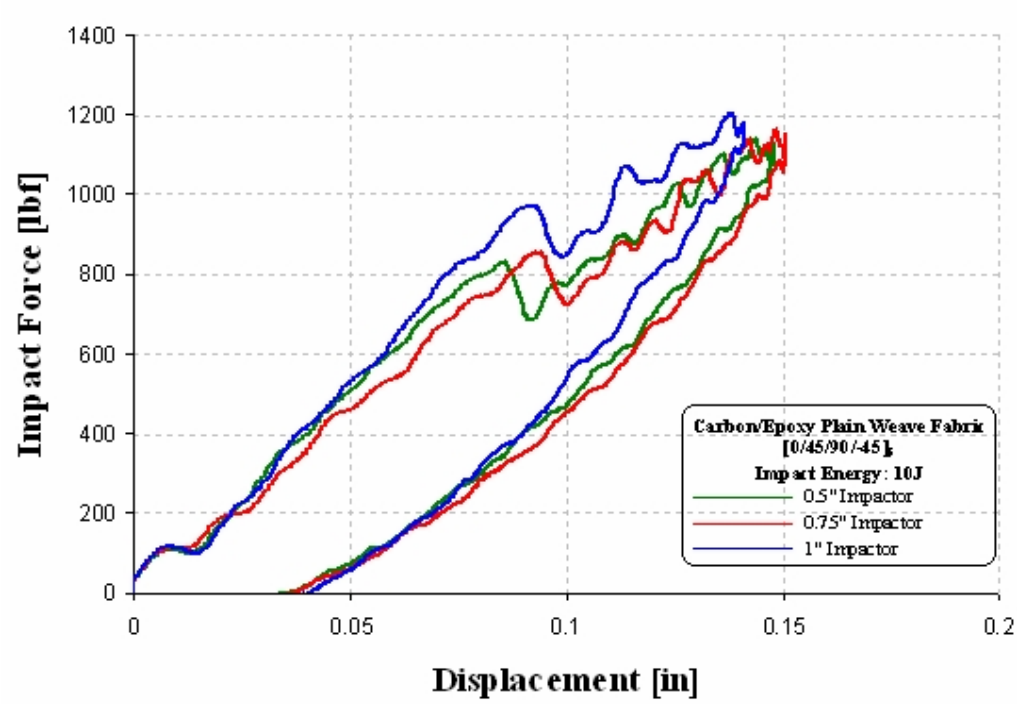

Figure 49. Typical Force Displacement plot of a carbon/epoxy plain weave test coupon impacted at 10J.

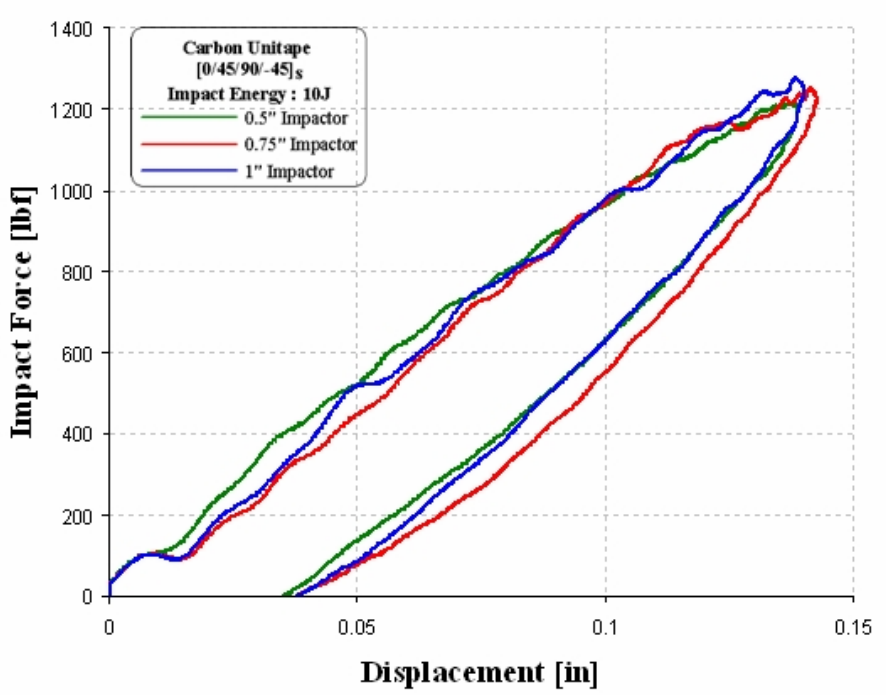

Figure 50. Typical Force Displacement plot of a carbon unitape test coupon impacted at 10J.

A.6 FORCE TIME PLOTS FOR TEST COUPONS IMPACTED AT 25J

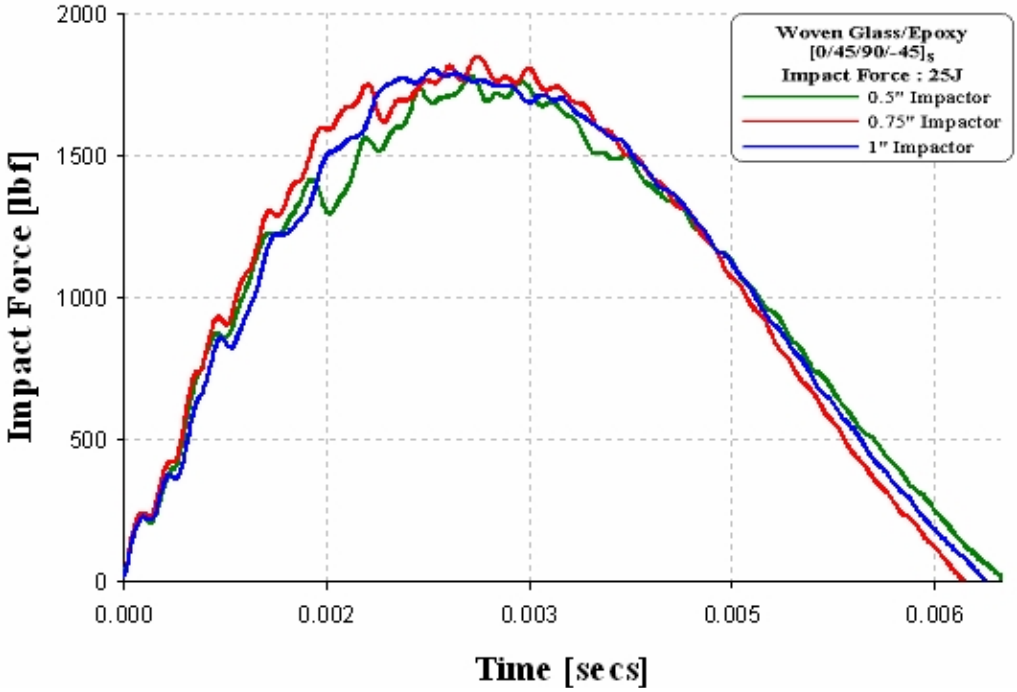

Figure 51. Typical Force Time plot of a woven glass/epoxy test coupon impacted at 25J.

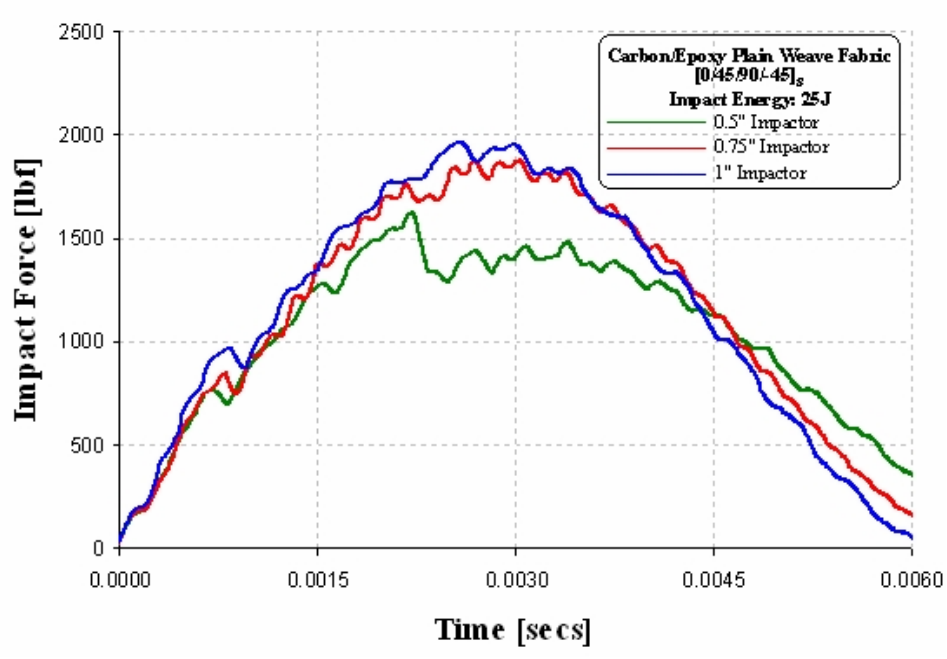

Figure 52. Typical Force Time plot of a carbon/epoxy plain weave test coupon impacted at 25J.

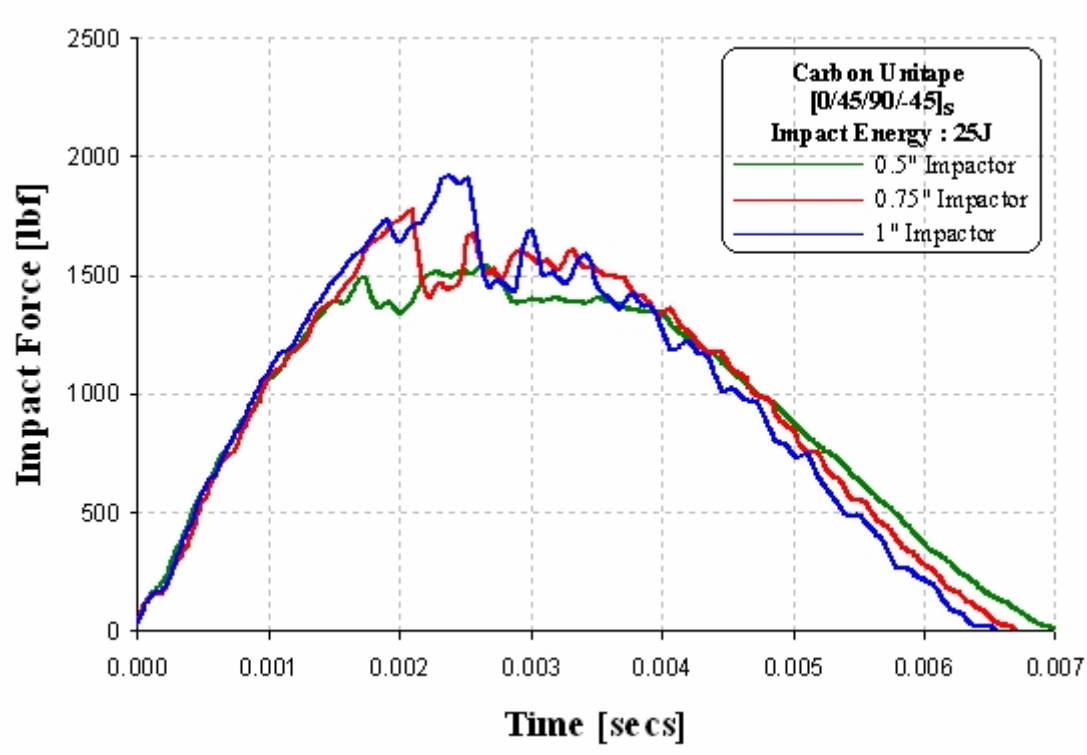

Figure 53. Typical Force Time plot of a carbon unitape test coupon impacted at 25J.

A.7 FORCE TIME PLOTS OF TEST COUPONS IMPACTED AT 10J

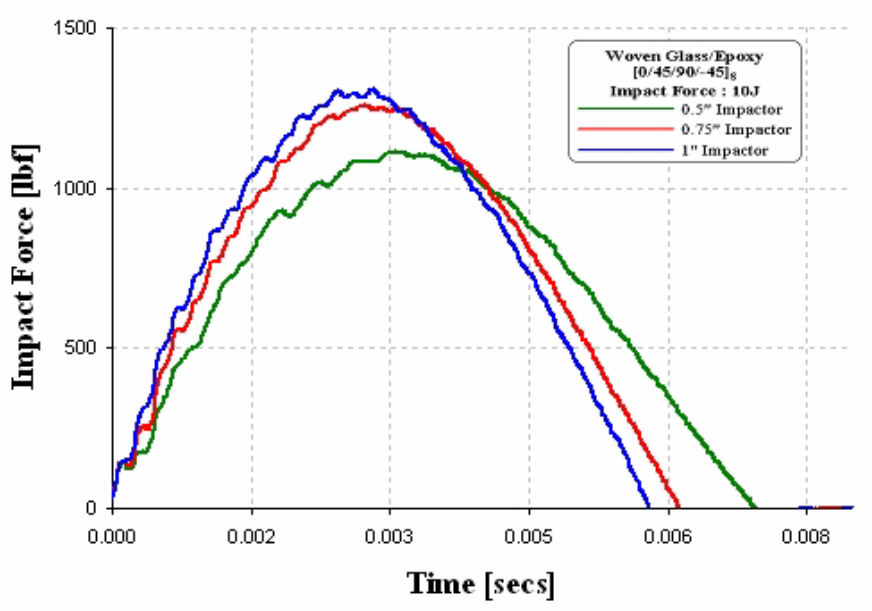

Figure 54. Typical Force Time plot of a woven glass/epoxy test coupon impacted at 10J.

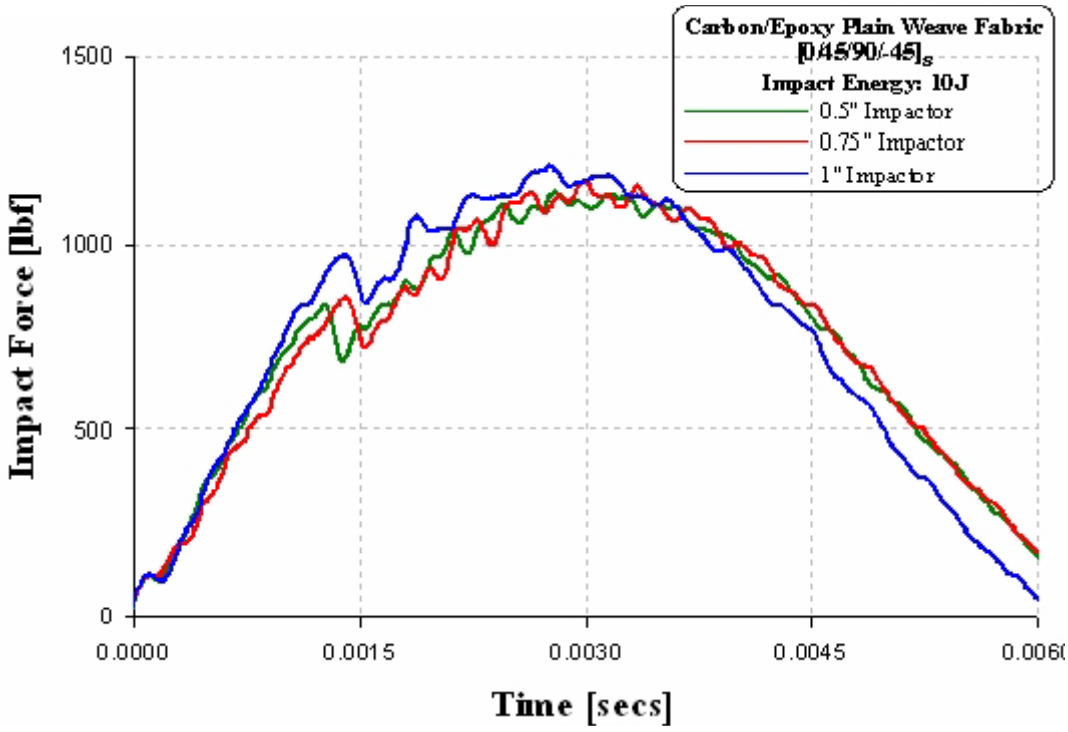

Figure 55. Typical Force Time plot of a carbon/epoxy plain weave test coupon impacted at 10J.

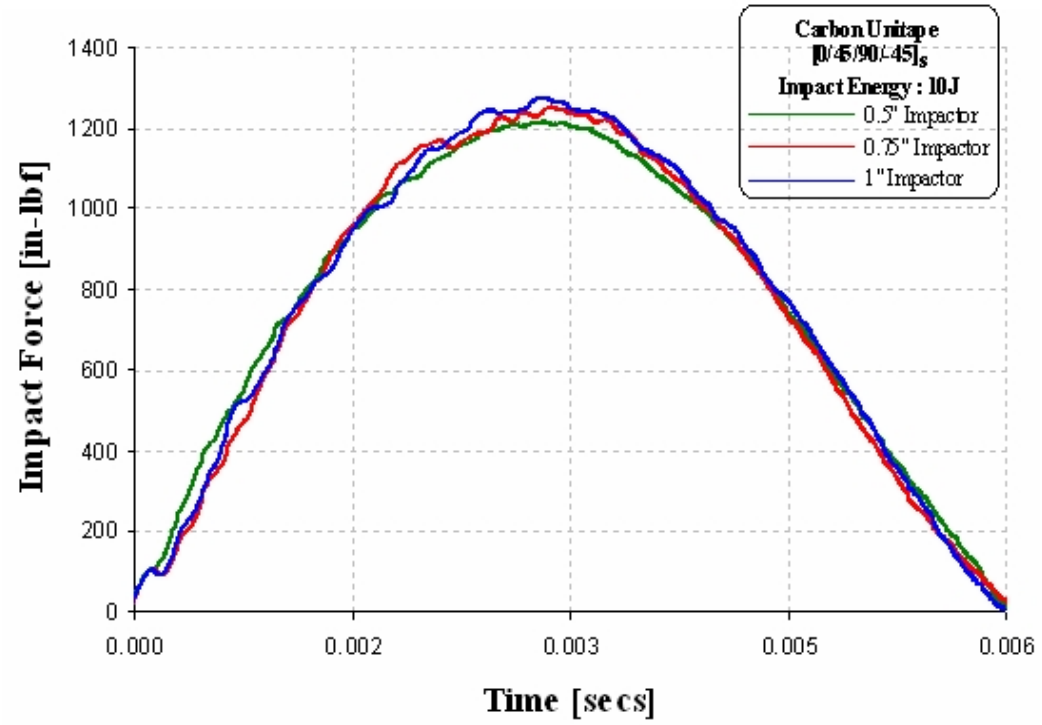

Figure 56. Typical Force Displacement plot of a carbon unitape test coupon impacted at 10J.

A.8 ENERGY TIME PLOTS OF TEST COUPONS IMPACTED AT 25J

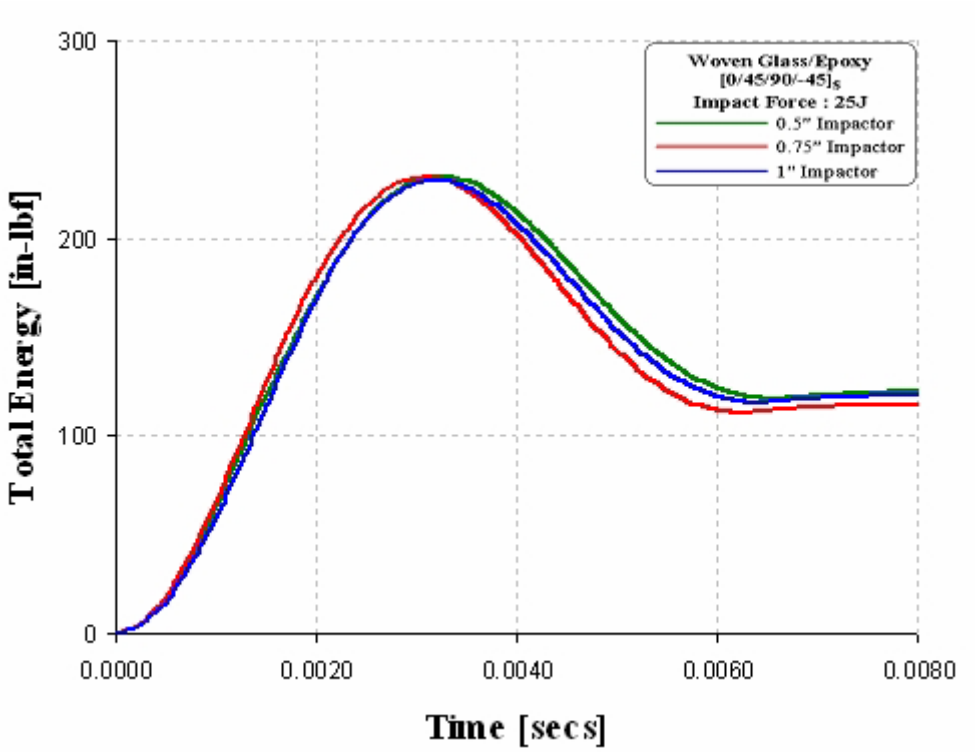

Figure 57. Typical Energy Time plot of a woven glass/epoxy test coupon impacted at 25J.

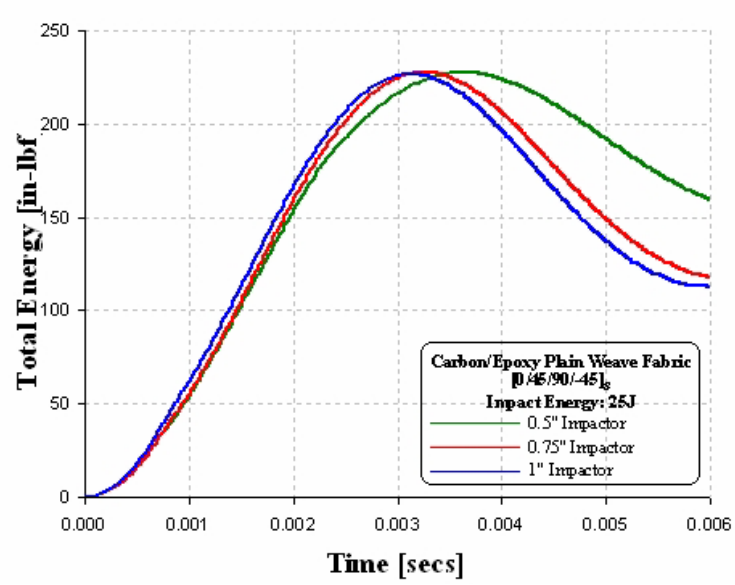

Figure 58. Typical Energy Time plot of a carbon/epoxy plain weave test coupon impacted at 25J

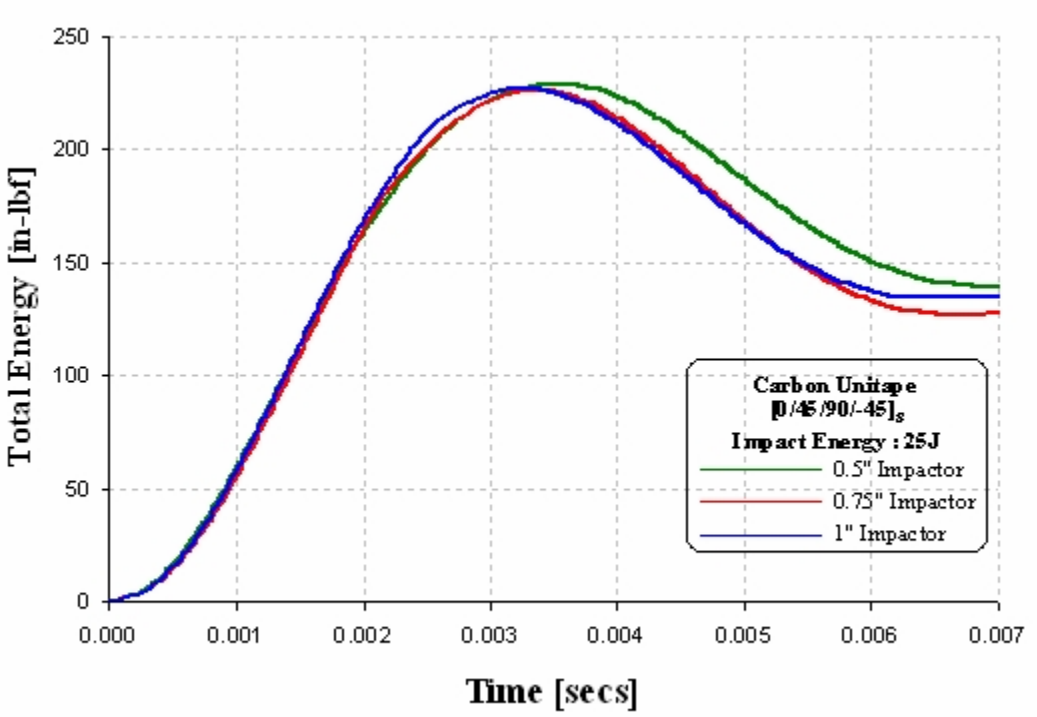

Figure 59. Typical Energy Time plot of a carbon unitape test coupon impacted at 25J.

A.9 ENERGY TIME PLOTS OF TEST COUPONS IMPACTED AT 10J

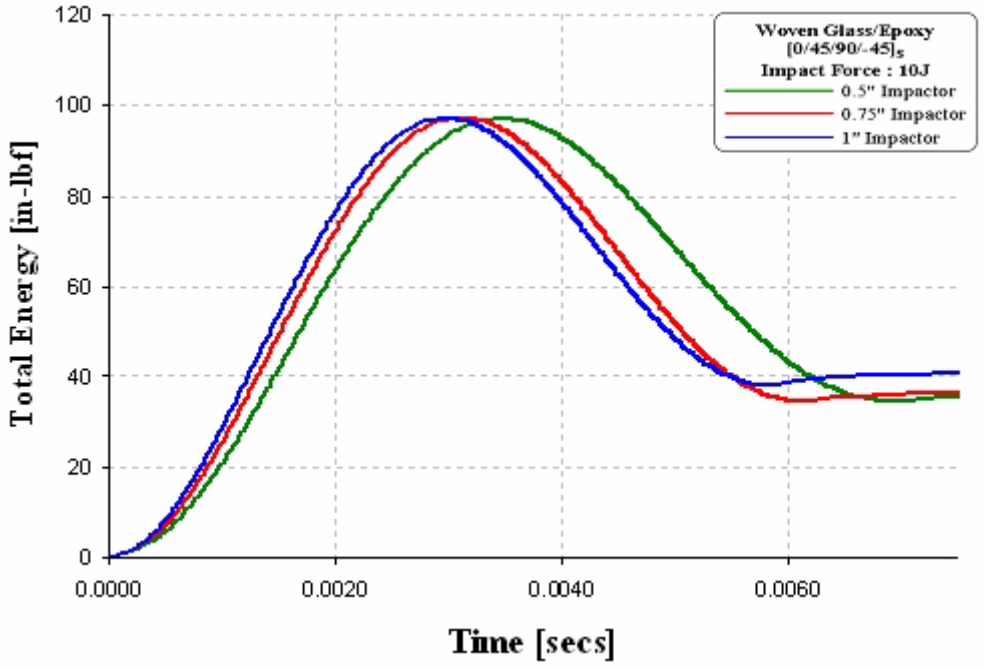

Figure 60. Typical Energy Time plot of a woven glass/epoxy test coupon impacted at 10J.

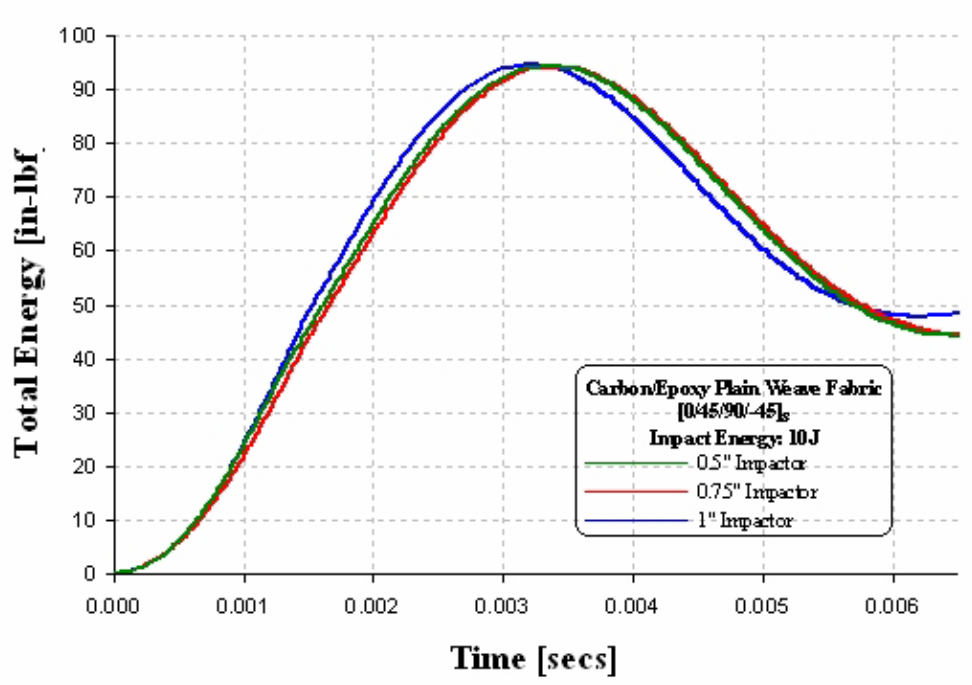

Figure 61. Typical Energy Time plot of a carbon/epoxy plain weave test coupon impacted at 10J.

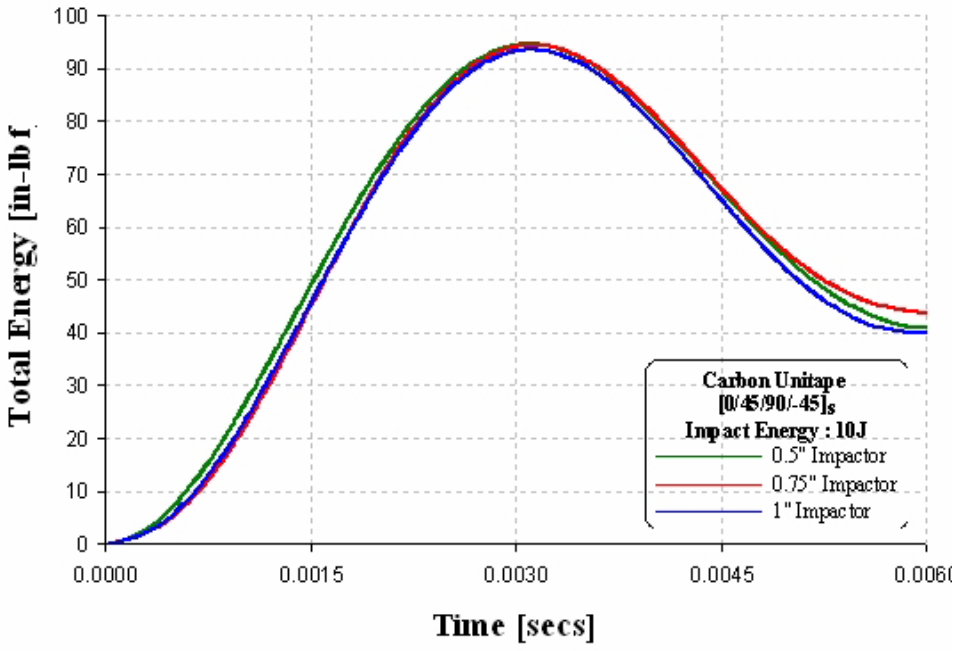

Figure 62. Typical Energy Time plot of a carbon unitape test coupon impacted at 10J.